Experimental and Kinetic Modeling Study of the Oxidation of Benzene

MARIA U. ALZUETA,* PETER GLARBORG, KIM DAM-JOHANSEN

Department of Chemical Engineering, Technical University of Denmark, 2800 Lyngby, Denmark

Received 16 November 1999; accepted 20 March 2000

ABSTRACT: The oxidation of benzene under flow-reactor conditions has been studied experimentally and in terms of a detailed chemical kinetic model. The experiments were performed under plug-flow conditions, at excess air ratios ranging from close to stoichiometric to very lean. The temperature range was 900–1450 K and the residence time of the order of 150 ms. The radical pool was perturbed by means of varying the concentration of water vapor and by adding NO. Furthermore, a few experiments were conducted on pyrolysis and oxidation of phenol. Benzene oxidation is initiated at ~1000 K; the temperature for complete oxidation depends on stoichiometry, ranging from 1100 K (very lean conditions) to 1300 K (close to stoichiometric). The water vapor level and the presence of NO have only a minor impact on the temperature regime for oxidation. The proposed chemical kinetic model was validated by comparison with the present experimental data as well as flow reactor and mixed reactor data from literature. The model provides a reasonably good description of the overall oxidation behavior of benzene over the range of conditions investigated. However, before details of the oxidation behavior can be predicted satisfactorily, a number of kinetic issues need to be resolved. These include product channels and rates for the reactions of phenyl and cyclopentadienyl with molecular oxygen as well as reaction chemistry for the oxygenated cyclic compounds formed as intermediates in the oxidation process. © 2000 John Wiley & Sons, Inc. Int J Chem Kinet 32: 498–522, 2000

INTRODUCTION

The oxidation chemistry of aromatic compounds is of significant theoretical and practical interest. Aromatic compounds are known to be harmful to the environment and the emission of these species from a number of combustion systems is a significant concern. Furthermore, aromatic species are important precursors to dioxins and to soot formation. Aromatic compounds are formed to some extent in most combustion processes; in addition, they are added in considerable quantities to unleaded gasolines in order to increase the octane number and prevent knock in engines.

The oxidation behavior of aromatic compounds is atypical compared to other hydrocarbons, due to the characteristics of the aromatic ring and its rupture. During the last two decades, significant experimental and theoretical efforts [1–19] have been aimed at improving our understanding of the oxidation behavior of these species. In his early review on aromatics oxidation, Brezinsky [4] identified a number of important unresolved issues. At present, more than a decade later, many of these issues remain unresolved. This can mainly be attributed to the complexity of the aromatics chemistry but also the limited availability of well-characterized experimental data has limited progress in our understanding. Large uncertainties still remain in the reaction mechanisms for even the simplest aromatic species, benzene and toluene.

Previous experimental studies dealing with benzene oxidation include flow reactor studies [2,4,6,7]; well-

Correspondence to: P. Glarborg (pgl@kt.dtu.dk)
*Present Address: Department of Chemical and Environmental Engineering, Centro Politecnico Superior, University of Zaragoza, 50015 Zaragoza, Spain

stirred reactor experiments [19]; shock tube CO data [3] and ignition delay data [5]; and low-pressure flame composition profiles [1,15] as well as flame speed measurements [16].

A number of modeling studies of benzene oxidation have been reported. In an early effort, Bittker [8] proposed a simplified mechanism to model the ignition delay time measurements of Burcat et al. [5] and the flow reactor data of Lovell et al. [6]. This mechanism was in part empirical, since the rate constants for a number of the most important reactions were adjusted to fit the experimental data. Based on the review [4] and flow-reactor experiments [6], Brezinsky and coworkers proposed the first detailed reaction mechanism for benzene and toluene oxidation [9]. This mechanism has been the starting point of most subsequent modeling studies, including those of Lindstedt and Skevis [10], Zhang and McKinnon [12], Tan and Frank [14], and Davis et al. [16]. In these studies, benzene oxidation mechanisms were tested against data from flames, mainly the low-pressure flame species profiles of Bittner and Howard [1]. In general, these comparisons confirm that important reaction paths are missing in the mechanism.

Progress in the understanding of the benzene oxidation chemistry has been facilitated by recent studies of important reaction subsets involving C_6 and C_5 species, [17,18,20–23] as well as the improved reliability of the C_1–C_4 hydrocarbon reaction subset [24–29]. The availability of thermodynamic properties is also enhanced [17,18,23,28,30,31], although significant uncertainties remain.

The objective of the present work is to perform an experimental and theoretical study of benzene oxidation under lean conditions and temperatures characteristic of postflame conditions. Perturbation experiments on benzene oxidation, supplemented with experiments on pyrolysis and oxidation of phenol, are carried out in an atmospheric pressure flow reactor in the temperature range 900–1400 K. Experimental data from the literature on flow reactor [6] and well-stirred reactor [19] experiments are also considered. A detailed reaction mechanism for the oxidation of benzene is proposed, and some important issues in our understanding of the oxidation benzene are discussed.

EXPERIMENTAL

The flow reactor and the experimental procedure are described elsewhere [32,33,34], and only a brief description is given here. A quartz flow reactor designed for obtaining plug flow in the laminar flow regime [32] was placed in a three-zone electrically heated oven, securing a uniform temperature profile within 10 K over the reactor. The reactor temperature was measured close to the reactor with a Type-K thermocouple.

The gaseous components were fed to the reactor in four separate streams. The main flow usually contained nitrogen and water vapor, and the rest of reactants were supplied through side injector tubes. In the experiments for analyzing phenol oxidation, phenol was dissolved in water and a nitrogen stream was saturated in the phenol solution at a given temperature. The inlet concentration of phenol was determined by complete oxidation at very lean conditions and high temperature (i.e., 50% O_2 and 1500 K). In most experiments, very diluted gas mixtures were used in order to maintain isothermal conditions along the reaction zone. The reactor tube used in the present experiments had a diameter of 0.89 cm and a length of 19 cm. The product gas was quenched at the outlet of the reactor by heat exchange with air.

The concentrations of CO, CO_2, O_2, and NO were measured continuously by spectrophotometric and paramagnetic analyzers, with an accuracy of $\pm 3\%$ but not less than 5 ppm. Furthermore, FTIR (Fourier-transformed infrared) spectra were taken, from which the concentrations of benzene have been determined. The uncertainty of these measurements has been estimated to be $\pm 10\%$ but not less than 10 ppm. The reactor pressure was measured with an absolute pressure transducer. Temperature control and data acquisition were automated, using a personal computer.

REACTION MECHANISM

The reaction mechanism for benzene oxidation developed in the present work consists of an oxidation subset for C_1–C_6 hydrocarbons, together with a small subset for reactions involving NO. The C_3–C_6 hydrocarbon subset is listed in Appendix A; the full reaction mechanism can be obtained directly from the authors in Chemkin format.

The model is an extension of the reaction mechanism developed for parabenzoquinone pyrolysis and oxidation by Alzueta et al. [22], drawing on the benzene oxidation scheme by Emdee et al. [9]. The C_5 hydrocarbon subset is mainly adopted from the recent work of Zhong and Bozzelli [17,18,35], while the C_3–C_4 hydrocarbon chemistry is based on the work of Miller and co-workers [24,27] and Marinov et al. [28]. The C_1–C_2/NO subset has been adopted without changes from Glarborg et al. [29].

The reverse rate constants were obtained from the forward rate constants and thermodynamic equilibrium constants. Thermodynamic data were taken

mostly from the Sandia Thermodynamic Database [30], Burcat and McBride [31], and Zhong and Bozzelli [17,18,35]. Appendix B lists thermodynamic properties (ΔH_{f298}, S_{f298}, and C_p) for selected species. The availability and accuracy of the aromatics' thermochemistry have improved considerably in recent years, but for a number of important intermediates, large uncertainties remain. The uncertainty in the heat of formation of C_6H_5 is now significantly reduced due to the work of Heckmann et al. [36], but large differences in reported data are still observed for species such as C_5H_5, C_5H_4O, and OC_6H_4O.

The elementary reactions in the oxidation scheme that are most important for the present calculations are discussed in detail next. The numbering of reactions corresponds to the listing in Appendix A. The discussion will focus mainly on the C_6/C_5 reaction subset, even though the chemistry of the smaller hydrocarbons also has some significance.

Under the conditions of the present study, the main consumption steps for benzene are the reactions with H, O, and OH radicals:

$$C_6H_6 + H \rightleftharpoons C_6H_5 + H_2 \qquad (-12)$$

$$C_6H_6 + O \rightleftharpoons C_6H_5O + H \qquad (1)$$

$$C_6H_6 + O \rightleftharpoons C_6H_5 + OH \qquad (2)$$

$$C_6H_6 + OH \rightleftharpoons C_6H_5 + H_2O \qquad (3)$$

$$C_6H_6 + OH \rightleftharpoons C_6H_5OH + H \qquad (-22)$$

The $C_6H_5 + H_2$ reaction (12) is well characterized both experimentally and theoretically [37], and the uncertainties for the reverse step, $C_6H_6 + H$, are mainly related to the thermochemistry of the phenyl radical. The product channels of the reaction of C_6H_6 with O atoms are still uncertain. The main reaction channel involves addition of an O atom to form a C_6H_6O adduct, which can follow either a rearrangement to produce phenol or suffer a ring hydrogen abstraction resulting in phenoxy. No quantitative measurements of the products have been reported. Earlier work [4,38] proposed the addition plus rearrangement channel leading to phenol as the preferred mechanism. Recently, Bajaj and Fontijn [39] concluded from a flow reactor study at 405 K that phenoxy is the main primary product of this step, although the formation of phenol cannot be excluded. Following Bajaj and Fontijn, we assume the phenoxy channel (1) to be dominating. The direct hydrogen abstraction by O radicals, reaction (2), is significantly slower than the addition reaction (1). We have adopted the rate constant estimated by Leidreiter and Wagner [40] from a shock tube study in the temperature range 1200–1450 K. The reaction of C_6H_6 with OH radicals proceeds mainly through hydrogen abstraction (3), even though the product channel forming phenol (−22) is almost as fast. The rate constants for these steps are accurate within a factor of two [26].

Reactions of the phenyl radical at elevated temperatures are not well characterized. Under lean conditions, C_6H_5 is mainly consumed by reaction with O_2. This reaction, a key step in aromatics oxidation and PAH growth [41,42], was until recently believed to be comparatively slow and to produce exclusively phenoxy radicals at higher temperatures [43]:

$$C_6H_5 + O_2 \rightleftharpoons C_6H_5O + O \qquad (13)$$

However, recent shock tubes studies by Frank et al. [20] and Kumaran and Michael [21] prove the $C_6H_5 + O_2$ reaction to be comparatively fast and indicate an important secondary channel producing H atoms:

$$C_6H_5 + O_2 \longrightarrow (\text{product}) + H \qquad (14a)$$

Both Frank et al. [20] and Kumaran and Michael [21] derived a branching ratio, k_{13}/k_{14a}, of about 3 under the conditions of their investigation (1000–1500 K), but no direct identification of the products of reaction (14a) could be made. Frank et al. proposed that the reaction formed parabenzoquinone, that is,

$$C_6H_5 + O_2 \rightleftharpoons pOC_6H_4O + H \qquad (14b)$$

This product channel was preferred to formation of the isomer orthobenzoquinone (oOC_6H_4O),

$$C_6H_5 + O_2 \rightleftharpoons oOC_6H_4O + H \qquad (14)$$

since parabenzoquinone is thermally more stable. The theoretical study on $C_6H_5O_2$ isomers by Mebel and Lin [44] is not conclusive regarding the products of the $C_6H_5 + O_2$ reaction, but indicates that several mechanisms may be involved.

In previous modeling studies [6,8,9,10,13,16], reaction (13) was the only product channel for the $C_6H_5 + O_2$ reaction. We have included the secondary H-forming channel, basing our choice of products on the fact that Chai and Pfefferle [19] detected only trace amounts of benzoquinone in their recent jet-stirred reactor study of lean benzene oxidation at 1000–1200 K. If formed as a major product in the $C_6H_5 + O_2$ reaction, parabenzoquinone would be expected to build up in considerable concentrations; pOC_6H_4O is comparatively stable at these temperatures [22]. For this reason, we presently consider formation of orthobenzoquinone (14) to be the most likely secondary

product channel of the phenyl + O_2 reaction. However, further work is clearly required in order to determine the products of this important reaction.

At lower temperatures, below 1000 K, addition of O_2 to phenyl followed by stabilization of $C_6H_5O_2$,

$$C_6H_5 + O_2 \rightleftharpoons C_6H_5O_2$$

is the dominant product channel [44,45,46]. However, in the shock tube studies at 1000–1500 K [20,21] no evidence of this reaction channel was found. A number of $C_6H_5O_2$ isomers may potentially be important at lower temperatures [44], but very little is known about thermochemistry and reaction pathways for these components. Based on the shock tube results, we have omitted formation and reactions of phenyl peroxy in the present mechanism, but further work is required to establish the importance of this species.

Other consumption steps for C_6H_5 include thermal dissociation, interaction with the radical pool, and reactions with aromatic and linear hydrocarbons. However, the impact of these reactions in the present calculations (stoichiometric to lean conditions) is small; phenyl is largely consumed by reaction with molecular oxygen.

Oxygenated aromatics such as phenol and phenoxy constitute important intermediates in benzene oxidation, and pathways through these components may lead to aromatic ring opening. A significant amount of recycling between C_6H_5OH and C_6H_5O may occur. Phenol is converted to C_6H_5O by reaction with the radical pool, mainly OH,

$$C_6H_5OH + OH \rightleftharpoons C_6H_5O + H_2O \qquad (24)$$

while phenoxy is recycled back to phenol mainly by the reactions

$$C_6H_5O + H \rightleftharpoons C_6H_5OH \qquad (16)$$

$$C_6H_5O + HO_2 \rightleftharpoons C_6H_5OH + O_2 \qquad (-25)$$

Overall this reaction sequence serves as a radical sink. The most important chain-terminating step is the C_6H_5O + H reaction (16), which proceeds close to collision frequency; the rate constant recommended by Baulch et al. [26] has been used. The rate constant for reaction (24) is also fairly well established [47], while for reaction (−25) an estimated rate for the reverse reaction was used, in the absence of measured data.

The recycle reactions compete with a number of steps that limit the size of the phenol/phenoxy pool. At higher temperatures, phenol and phenoxy may dissociate through CO elimination,

$$C_6H_5OH \rightleftharpoons C_5H_6 + CO \qquad (20)$$

$$C_6H_5O \rightleftharpoons C_5H_5 + CO \qquad (15)$$

Shock tube experiments on phenol pyrolysis experiments [48] indicate that (20) is the major dissociation pathway, with a secondary channel forming phenoxy and H atoms (−16). However, the importance of reaction (20) has been questioned [15] , based on results from modeling low-pressure benzene flames. This issue is discussed further later.

For thermal decomposition of C_6H_5O (15), we have adopted the measurement of Frank et al. [20]. Recent theoretical studies [49,50] indicate that the activation energy for this reaction should be considerably higher than the value of approximately 44 kcal/mol inferred experimentally [20,43]; this issue needs to be addressed.

Phenoxy may also lead to benzoquinone by reaction with O atoms,

$$C_6H_5O + O \rightleftharpoons pOC_6H_4O + H \qquad (17)$$

$$C_6H_5O + O \rightleftharpoons oOC_6H_4O + H \qquad (18)$$

According to the work of Buth et al. [51], the C_6H_5O + O reaction is very fast, producing benzoquinone and H atoms [51]. The branching fraction between the two potential product channels (17, 18) is uncertain; as a first approximation we have assumed that the two benzoquinone isomers are formed in equal quantities. The formation of the two benzoquinone isomers is supported by the *ab initio* study of Lin and Mebel [52]; it is noteworthy, however, that Lin and Mebel predict a much lower reaction rate than that determined experimentally by Buth et al.

The benzoquinone isomer, which has been detected as intermediate in benzene oxidation [19], is presumably parabenzoquinone; orthobenzoquinone is not thermally stable, as we will discuss. In a previous flow reactor study [22], we analyzed the chemistry of this compound under pyrolysis and oxidation conditions. In the temperature range of the present study, dissociation is a key step in parabenzoquinone consumption, both under pyrolysis and oxidation conditions. The main dissociation pathway is [20,22],

$$pOC_6H_4O \rightleftharpoons C_5H_4O + CO \qquad (31)$$

but also a secondary channel may be active [22],

$$pOC_6H_4O \rightleftharpoons C_5H_4 + CO_2 \qquad (32)$$

At high temperatures and lean conditions, reactions of

p-OC_6H_4O with the radical pool become significant. The main steps are proposed to be [22],

$$p\text{-}OC_6H_4O + H \rightleftharpoons C_5H_5O + CO \quad (33)$$

$$p\text{-}OC_6H_4O + H \rightleftharpoons OC_6H_3O + H_2 \quad (34)$$

$$p\text{-}OC_6H_4O + O \longrightarrow C_6H_3O_3 + H \quad (35)$$

$$p\text{-}OC_6H_4O + O \rightleftharpoons OC_6H_3O + OH \quad (36)$$

$$p\text{-}OC_6H_4O + OH \rightleftharpoons OC_6H_3O + H_2O \quad (37)$$

Subsequently, $C_6H_3O_3$ and OC_6H_3O are assumed to react by dissociation or reaction with the radical pool (38–42), leading to ring opening [22]. Details of the reaction subset for parabenzoquinone are still uncertain, but the overall pyrolysis and oxidation behavior is fairly well described [22].

Orthobenzoquinone, if formed in reactions (14) or (18), would be expected to react differently from parabenzoquinone. Orthobenzoquinone dissociates readily even at comparatively low temperatures. De Jongh et al. [53] reported thermolysis of o-OC_6H_4O to be very fast at 1073 K, with the major product being cyclopentadienone (detected as the dimer),

$$o\text{-}OC_6H_4O \rightleftharpoons C_5H_4O + CO \quad (30)$$

The rapid dissociation of o-OC_6H_4O and the formation of C_5H_4O as the major product have been confirmed by subsequent studies [54]. The lower thermal stability of o-OC_6H_4O compared to p-OC_6H_4O is in agreement with the general observation that *o*-quinones are decarbonylated more readily than *p*-quinones [55]. In the absence of direct measurements for the rate constant of (30), we employ an estimated value for this exothermic reaction. Our estimated activation energy corresponds roughly to the C—C bond strength between the two carbonyl elements in o-OC_6H_4O, which is about 40.6 kcal/mol [54]. With this rate constant, o-OC_6H_4O dissociates readily under the conditions investigated in the present study, and no other reactions for this component were included in the mechanism.

Cyclopentadiene (C_5H_6) and the derived radical, cyclopentadienyl (C_5H_5), are major intermediates formed in the high-temperature oxidation of benzene, and their fate is critical for the oxidation process. Recent studies of the pyrolysis [23,56,57,58] and oxidation [56] of cyclopentadiene have improved our knowledge of the chemistry of these components, but significant uncertainties remain, both in their reaction mechanism and in the thermochemistry of these important intermediates.

The cyclopentadiene reaction subset used in previous models has generally relied on the estimates of Emdee et al. [9]. Due to the comparatively weak bonding of the hydrogen atoms, Emdee et al. assumed that the consumption of C_5H_6 occurred largely through hydrogen abstraction reactions, mainly

$$C_5H_6 + H \rightleftharpoons C_5H_5 + H_2 \quad (49)$$

$$C_5H_6 + O \rightleftharpoons C_5H_5 + OH \quad (53)$$

$$C_5H_6 + OH \rightleftharpoons C_5H_5 + H_2O \quad (55)$$

$$C_5H_6 + HO_2 \rightleftharpoons C_5H_5 + H_2O_2 \quad (57)$$

$$C_5H_6 + O_2 \rightleftharpoons C_5H_5 + HO_2 \quad (58)$$

The rate coefficients were estimated by analogies to CH_2O reactions [9]. The recent theoretical work of Zhong and Bozzelli [17] indicates, however, that a number of addition reactions compete with the metathesis steps. Zhong and Bozzelli predict from QRRK theory that a significant fraction of the cyclopentadiene may react to form oxygenated compounds and propose a number of oxidation pathways not considered in previous modeling studies. These reactions, which in general have not been characterized experimentally, limit formation of the cyclopentadienyl radical and open up a number of alternative ring-opening oxidation pathways.

For most of the abstraction reactions (53, 55, 57, 58), rate constants still rely on estimates (Appendix A). Only for the C_5H_6 + H reaction (49) are experimentally determined rate coefficients now available [56]. For the addition reactions discussed next, experimental data are also very limited; we largely rely on the QRRK estimates of Zhong and Bozzelli [17,18].

The C_5H_6 + H abstraction reaction (49) competes with addition of the hydrogen atom to the double bond in C_5H_6, resulting mainly in stabilization of C_5H_7 [17], either the cyclic isomer,

$$C_5H_6 + H \rightleftharpoons C_5H_7 \quad (50)$$

or, after ring opening, a linear isomer,

$$C_5H_6 + H \rightleftharpoons CH_2CH\dot{C}HCHCH_2 \quad (51)$$

Addition of an oxygen atom to C_5H_6 leads mainly to formation of cyclic C_5H_5O [17]:

$$C_5H_6 + O \rightleftharpoons C_5H_5O + H \quad (52)$$

In the present work, no distinction is made between the cyclic C_5H_5O isomers formed in this reaction. Addition of OH to cyclopentadiene leads to a linear alcohol [17]:

$$C_5H_6 + OH \rightleftharpoons CH_2CH\dot{C}HCHCHOH \quad (54)$$

while addition of HO_2 to C_5H_6 mainly results in a cyclic C_5H_7 radical and O_2:

$$C_5H_6 + HO_2 \rightleftharpoons C_5H_7 + O_2 \qquad (56)$$

The cyclopentadienyl radical (C_5H_5), which is an important intermediate in the transition from cyclic to linear chain kinetics, is a resonance-stabilized radical. It has been assumed to be consumed mainly through radical/radical reactions with the O/H radical pool [4]. However, reaction with molecular oxygen [18] or isomerization to its linear form [56,58] have also been suggested to be important.

The reactions of C_5H_5 with H and O radicals have been extensively studied in recent years [18,21,56,58, 59]. The $C_5H_5 + H$ reaction,

$$C_5H_5 + H \rightleftharpoons C_5H_6 \qquad (66)$$

has been measured in both forward and reverse directions, and the rate constant is fairly well established. Reported data [21,59] agree within a factor of 2 at a temperature of 1100 K, ranging from $1.0 \cdot 10^{14}$ to $2.0 \cdot 10^{14}$ cm^3/mols.

Similarly, to $C_5H_5 + H$, the reaction of C_5H_5 with O radicals proceeds close to collision frequency. Shock tube studies [20,21] indicate that the major product channel involves formation of H atoms:

$$C_5H_5 + O \rightleftharpoons C_5H_4O + H \qquad (68)$$

Zhong and Bozelli [18] confirm reaction (68) as the main product channel but identify also a second reaction pathway, involving ring opening:

$$C_5H_5 + O \rightleftharpoons CH_2CHCH\dot{C}H + CO \qquad (67)$$

The association of hydroxyl radicals to the cyclopentadienyl radical,

$$C_5H_5 + OH \rightleftharpoons (C_5H_5OH) \qquad (69)$$

is proposed to result in an energized cyclopentadienol radical [18]. This adduct can stabilize or isomerize to cyclopentadiene-1-ol and cyclopentadiene-2-ol. According to the QRRK calculations [18], these three exothermic product channels have comparable reaction rates. In the mechanism, we do not distinguish between these isomers. The channel leading to the cyclopentadienol and H,

$$C_5H_5 + OH \rightleftharpoons C_5H_4OH + H \qquad (70)$$

which in previous models was assumed to be the major reaction pathway, is endothermic and significantly slower [18].

As discussed by Zhong and Bozzelli [18], the reaction of C_5H_5 with HO_2 may be a key reaction in the lean oxidation of benzene. Both of these radicals are comparatively unreactive and may build up to relatively large concentrations. The addition of hydroperoxy radical to C_5H_5 forms a complex, which either dissociates, liberating OH radicals or a water molecule, or recycles back to reactants. The dominating product channel appears to be

$$C_5H_5 + HO_2 \rightleftharpoons C_5H_5O + OH \qquad (71)$$

This reaction is comparatively fast and will act as a pseudochain branching step in the oxidation process.

The reaction of the cyclopentadienyl radical with molecular oxygen has been suggested to be a major consumption route for C_5H_5 [2,56], but little is known about it. Roy and Frank [56] suggest that the reaction mainly produces C_5H_4O:

$$C_5H_5 + O_2 \rightleftharpoons C_5H_4O + OH$$

and derive a set of rate coefficients with a very high preexponential factor from shock tube measurements. QRRK calculations [18] indicate that the addition of O_2 to C_5H_5 forms an energized peroxy radical, which predominantly dissociates back to reactants. However, a minor fraction of the adduct formed may undergo a ring-opening reaction [18]:

$$C_5H_5 + O_2 \rightleftharpoons CH_2CHCHCO + HCO \qquad (72)$$

Despite a low reaction rate, about two orders of magnitude lower than the value derived by Roy and Frank, this step may consume a significant fraction of the cyclopentadienyl under lean conditions and thus acts as an important path for the conversion of cyclopentadienyl radical into linear species.

The fate of the cyclic compounds formed from C_5H_5 and C_5H_6 (i.e., C_5H_5OH, C_5H_5O, C_5H_4OH, and C_5H_4O) is uncertain. There are no indications either in the present experimental work or from results reported in literature that any of these components build up to significant concentrations during benzene oxidation, not even in the 1000–1200 K range. Presumably, C_5H_5O and C_5H_4OH dissociate fairly rapidly, while C_5H_5OH and C_5H_4O are thermally more stable. In particular, reactions of cyclopentadienone are important, since this species appears to be an important link between the aromatic and nonaromatic hydrocarbons during the benzene oxidation process. Emdee et al.

[9] assumed C_5H_4O to open and lose the CO group according to

$$C_5H_4O \longrightarrow C_2H_2 + C_2H_2 + CO \qquad (86)$$

In a more recent work, Wang and Brezinsky [23] proposed, based on molecular orbital and RRKM theory, that the thermal dissociation of cyclopentadienone leads mainly to cyclobutadiene:

$$C_5H_4O \longrightarrow cC_4H_4 + CO \qquad (86a)$$

with a rate constant in fairly good agreement with the early estimate [9]. In the present work, we have adopted the rate constant estimated by Wang and Brezinsky but assume cyclobutadiene to dissociate readily to acetylene. However, dissociation of C_5H_4O has a large activation energy due to the endothermicity of the reaction and is fairly slow under the conditions of interest in the present study. If reaction (86) is used as the main consumption step for cyclopentadienone, as proposed by Emdee and co-workers, C_5H_4O builds up to large concentrations in our modeling predictions. This is in contrast to the present experimental data set as well as the data of Chai and Pfefferle [19]. We have added a subset for reactions of cyclopentadienone with the radical pool (reactions 87–91), either hydrogen abstraction (analogy with benzene steps) or ring opening. However, even with very fast rates, these reactions do not prevent C_5H_4O from accumulating under certain conditions in our calculations.

Results from thermal decomposition of C_5H_4O precursors, oOC_6H_4O [53] and dihydro-benzodioxin [54], show that cyclopentadienone is rapidly consumed, even at low temperatures (850–1100 K) and low radical concentrations. The fast consumption of C_5H_4O under these conditions was attributed to a fast dimerization reaction; while no or small amounts of C_5H_4O were detected, the dimer or decomposition/rearrangement products from the dimer were identified [53,54]. Based on their results, Schraa et al. [54] derived a very fast dimerization rate for C_5H_4O, $4.0 \cdot 10^{11}$ cm^3/mol-s at 850 K, a value much higher than for other Diels-Alder reactions. Whether or not this very high value can be confirmed, the results indicate a high reactivity of cyclopentadienone.

In flames, cyclopentadienone is consumed rapidly by thermal dissociation (86), but in the temperature range of the flow reaction (i.e., 1000–1400 K) and jet-stirred reactor studies, this step is too slow to account for the consumption of C_5H_4O. Due to the lack of detailed kinetic information, Tan and Frank [14] described C_5H_4O consumption in terms of a global reaction step:

$$C_5H_4O \longrightarrow C_4H_4 + CO \qquad (86b)$$

Since a large fraction of the oxidation route for benzene appears to proceed through cyclopentadienone under the conditions of the present study, such a global consumption step would have significant implications for the predicted oxidation behavior. We have chosen not to include such an overall reaction; however, clearly the development of a reliable aromatics oxidation mechanism requires a better characterization of the reactions of C_5H_4O.

The ring rupture of the cyclic compounds results in a number of linear C_4 and C_5 hydrocarbons, some of which are oxygenated. Very few reactions of these species have been characterized experimentally, and this subset of the mechanism relies largely on QRRK estimates [35] or estimates based on analogies with C_1–C_3 hydrocarbon reactions. Even though few of these reactions show up in sensitivity analyses for benzene oxidation under the present conditions, the uncertainties in the C_3–C_5 subset limit the reliability of the model predictions and will have to be dealt with in further work. Another potential limitation of the mechanism is that formation of polyaromatic compounds and hydrocarbons higher than C_6 was not considered. Even under slightly lean conditions, such species have been detected in minor concentrations [19], and they may affect the benzene oxidation chemistry.

RESULTS AND DISCUSSION

The oxidation of benzene has been studied in the temperature range 900–1400 K at atmospheric pressure in a flow reactor. The experiments were conducted keeping a constant mass flow rate and varying the reaction temperature. This means that the residence time in the reactor is a function of temperature, being about 150 ms at 1200 K. The benzene experiments were performed as perturbation studies, varying the oxygen concentration between 800 ppm and 50% (corresponding to excess-air ratios ranging from about stoichiometric to 600); the concentration of water vapor (0.5 and 5%); and the concentration of NO (0 and 100 ppm). In addition to the benzene experiments, a few experiments were performed to study the pyrolysis and oxidation of phenol. Table I shows the experimental matrix.

To complement the experimental data obtained in the present study, additional flow reactor data from Lovell et al. [6] and well-stirred reactor data from Chai and Pfefferle [19] were analyzed. In these studies, a smaller range of reaction conditions was covered, but contrary to the present study, concentrations of impor-

Table I Experimental Conditions*

Set	C_6H_6 (ppm)	C_6H_5OH (ppm)	O_2 (ppm)	λ	H_2O (%)	NO (ppm)	Residence time (s)
1		50	trace		2.00	0	165[K]/*T*
2		28	250000	1275	4.70	0	115[K]/*T*
3	111		870	1.04	0.53	0	178[K]*T*
4	106		830	1.04	0.51	104	180[K]/*T*
5	107		1290	1.60	4.87	0	185[K]/*T*
6	102		1226	1.60	4.65	101	177[K]/*T*
7	105		39100	49.6	0.50	0	181[K]/*T*
8	101		37400	49.4	0.47	109	173[K]/*T*
9	108		39100	48.3	4.70	0	187[K]/*T*
10	109		38800	47.4	4.70	139	186[K]/*T*
11	110		491000	600	1.23	0	184[K]/*T*

* The experiments are conducted at constant mass flow, and thereby the residence time is dependent on the reaction temperature, as listed. The pressure in the experiments is 1.05 bar.

tant intermediate species formed during benzene oxidation were measured. The significant range of conditions covered by the experimental data allows an assessment of the model capabilities, but a thorough validation of the reaction mechanism would require a more comprehensive characterization of stable and intermediate species.

The model calculations were performed using Senkin [60] for plug-flow calculations and PSR [61] for well-stirred reactor modeling; both of these codes run in conjunction with the Chemkin library [62].

Phenol Experiments

Phenol is an important intermediate during the combustion of aromatics [48,63], but it was not possible to measure the concentration of this component in our benzene oxidation experiments. As we will discuss, the present reaction mechanism describes satisfactorily the phenol profile in the benzene oxidation flow-reactor experiments of Lovell et al. [6] but grossly overpredicts the phenol concentration under the stirred-reactor conditions of the experiments of Chai and Pfefferle [19]. For this reason, we performed separate experiments to study the pyrolysis and the oxidation of phenol in the temperature range 900–1450 K. Thereby, the phenol chemistry subset of the model could be evaluated independently of the benzene reactions.

Figure 1 compares experimental (symbols) and predicted (lines) concentrations of CO and CO_2 from pyrolysis of phenol. In addition to phenol and nitrogen, the inlet gas contained about 2% of water vapor (Table I, Set 1). Oxygen impurities may be present in the re-

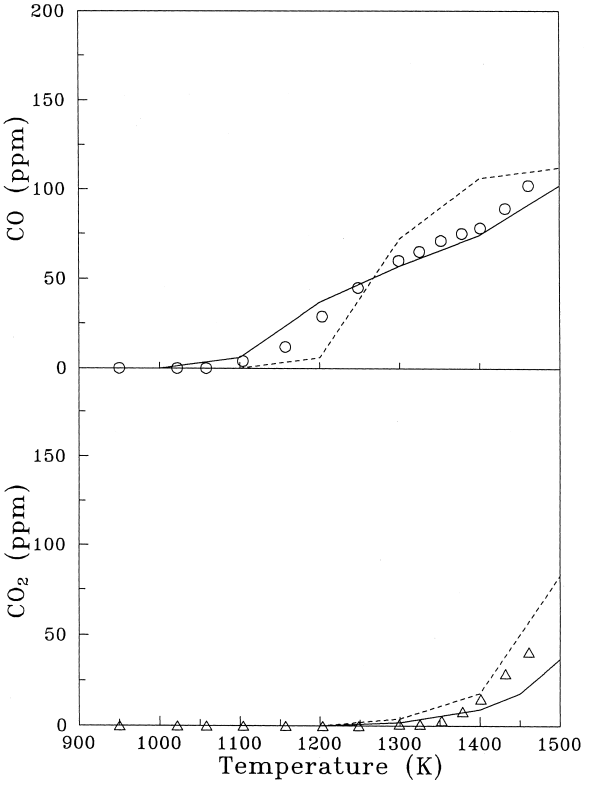

Figure 1 Comparison between experimental data and model predictions for CO and CO_2 during pyrolysis of phenol as function of temperature. Solid lines denote model predictions with the Appendix A mechanism; dashed lines denote calculations without the reaction $C_6H_5OH \rightleftharpoons C_5H_6 + CO$ (20). The inlet conditions are listed as Set 1 in Table I.

actant mixture in trace amounts (10–50 ppm) due to oxygen dissolved in the aqueous solution of phenol. However, from kinetic modeling calculations we conclude that the oxygen impurities are much lower than 50 ppm.

Formation of CO occurs at temperatures higher than 1100 K and increases monotonically with temperature. No maximum in CO is attained for the conditions studied. At the highest temperatures, CO_2 is also formed. Also, a number of intermediate species are formed; FTIR spectra indicate the presence of significant amounts of CH_4 and C_2H_2, as well as other unidentified species.

Model predictions performed with the Appendix A mechanism are shown as solid lines on Figure 1. The onset and profile of both CO and CO_2 are well predicted by the model. The calculations indicate that the formation of CO_2 is due to the presence of water and the subsequent H/O radical pool generated.

There is some controversy regarding the primary product channel for phenol dissociation. The chain initiation channel to phenoxy and H,

$$C_6H_5OH \rightleftharpoons C_6H_5O + H \qquad (-16)$$

is well established, through measurements in the reverse direction. A product channel forming cyclopentadiene and carbon monoxide,

$$C_6H_5OH \rightleftharpoons C_5H_6 + CO \qquad (20)$$

was proposed by Cyprès and Bettens [64] from isotope-marked experiments around 1000 K. This product channel was later confirmed by Horn et al. [48] based on H and CO concentration profiles in phenol pyrolysis shock tube experiments. However, Shandross et al. [15] found channel (20) to be inconsistent with data from low-pressure benzene flames.

A first-order sensitivity analysis for CO in phenol pyrolysis under the conditions of Figure 1 is shown in Table II. The analysis predicts a high sensitivity of the predicted CO concentration towards the rate constant of reaction (20). However, this is an artifact of the sensitivity analysis; as pointed out recently by Brezinsky et al. [65], flow-reactor results for CO (or C_5H_6) cannot distinguish between the phenol dissociation channels, since both channels ultimately lead to the same set of stable species. Reaction (20) corresponds to the reaction sequence $C_6H_5OH \rightleftharpoons C_6H_5O + H$ (-16), $C_6H_5O \rightleftharpoons C_5H_5 + CO$ (15), and $C_5H_5 + H \rightleftharpoons C_5H_6$ (66). This is confirmed by the results of Figure 1, where the dashed lines denote modeling predictions excluding reaction (20). The difference between the two sets of calculations is too small to distinguish between the dissociation channels of phenol, considering the uncertainty in secondary reactions.

We have chosen to retain reaction (20) in the reaction mechanism, since the shock tube measurements of Horn et al. [48] are considered to be more sensitive to the phenol dissociation products than the low-pressure benzene flames [15].

Figure 2 shows results for oxidation of phenol under very lean conditions. The formation of CO is initiated at temperatures above 950 K and reaches its maximum concentration at about 1100 K. At temperatures above 1200 K, all the phenol is oxidized to CO_2. The model predictions are in good agreement with the experimental results. Under the conditions studied, phenol is mainly consumed by hydrogen abstraction reactions:

$$C_6H_5OH + OH \rightleftharpoons C_6H_5O + H_2O \qquad (24)$$

$$C_6H_5OH + O \rightleftharpoons C_6H_5O + OH \qquad (23)$$

$$C_6H_5OH + HO_2 \rightleftharpoons C_6H_5O + H_2O_2 \qquad (26)$$

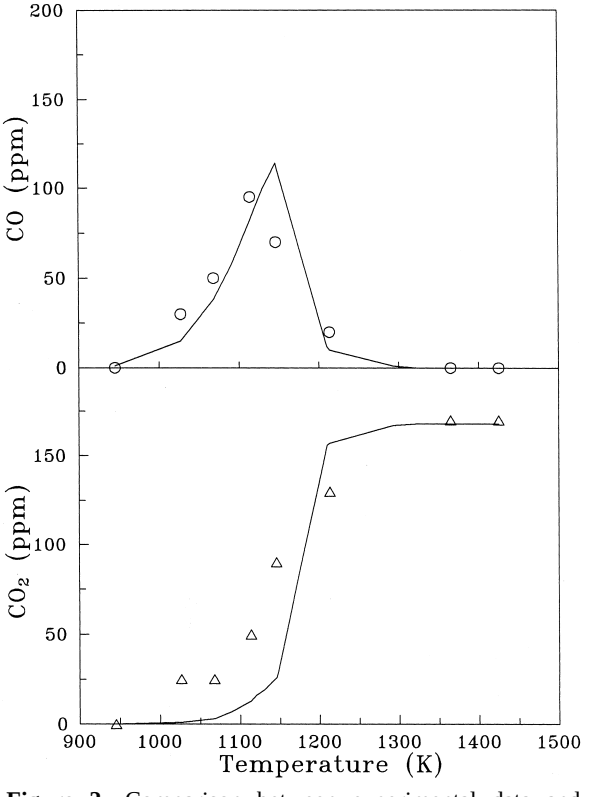

Figure 2 Comparison between experimental data and model predictions for CO and CO_2 during oxidation of phenol as function of temperature. The inlet conditions are listed as Set 2 in Table I.

Table II Linear Sensitivity Coefficients for CO at Initiation Conditions for Selected Sets of Conditions*

Reaction	Set 1 1150 K	Set 2 1025 K	Set 3 1050 K	Set 5 1000 K	Set 7 975 K	Set 9 950 K	Set 4 1000 K	Set 10 900 K
1. $C_6H_6 + O \rightleftharpoons C_6H_5O + H$			−0.08	−0.21	−0.21	−1.58	−0.16	0.03
2. $C_6H_6 + O \rightleftharpoons C_6H_5 + OH$					0.07	0.02		
3. $C_6H_6 + OH \rightleftharpoons C_6H_5 + H_2O$			0.25	0.51	1.19	1.33	0.47	0.64
12. $C_6H_5 + H_2 \rightleftharpoons C_6H_6 + H$			0.05	0.02			0.02	
13. $C_6H_6 + O_2 \rightleftharpoons C_6H_5O + O$			0.03	0.11	0.27	0.47	0.11	−0.01
14. $C_6H_5 + O_2 \rightleftharpoons oOC_6H_4O + H$			−0.02	−0.07	−0.27	−0.47	−0.07	0.02
15. $C_6H_5O \rightleftharpoons C_6H_5 + CO$		0.24	0.19	0.37	1.37	1.04	0.28	0.74
16. $C_6H_5O + H \rightleftharpoons C_6H_5OH$	0.02		0.17	−0.28	−0.24	−0.19	−0.23	−0.51
17. $C_6H_5O + O \rightleftharpoons pC_6H_4O + H$			0.01	−0.05	−0.21	−0.23	−0.04	−0.20
18. $C_6H_5O + O \rightleftharpoons oC_6H_4O + H$				−0.01	0.08	−0.12	−0.02	0.04
20. $C_6H_5OH \rightleftharpoons C_5H_6 + CO$	0.92	0.06						
22. $C_6H_5OH + H \rightleftharpoons C_6H_6 + OH$			−0.06	−0.15	−0.15	−0.37	−0.14	0.12
24. $C_6H_5OH + OH \rightleftharpoons C_6H_5O + H_2O$		0.20	−0.02	−0.07	−0.04	−0.05	−0.06	−0.14
25. $C_6H_5OH + O_2 \rightleftharpoons C_6H_5O + HO_2$		0.78		−0.01	−0.13	−0.21		−0.03
26. $C_6H_5OH + HO_2 \rightleftharpoons C_6H_5O + H_2O_2$		0.20						
49. $C_5H_6 + H \rightleftharpoons C_6H_5 + H_2$			−0.07	−0.02			−0.01	
58. $C_5H_6 + O_2 \rightleftharpoons C_5H_5 + HO_2$		0.02	−0.01	−0.01	−0.01	−0.61		
66. $C_5H_5 + H \rightleftharpoons C_5H_6$			−0.56	−0.28	−0.01		−0.31	−0.01
68. $C_5H_5 + O \rightleftharpoons C_5H_4O + H$			−0.02	−0.04	−0.02		−0.05	−0.03
69. $C_5H_5 + OH \rightleftharpoons C_5H_5OH$			−0.05	−0.10	−0.01		−0.11	−0.01
71. $C_5H_5 + HO_2 \rightleftharpoons C_5H_5O + OH$		0.05	0.10	0.08	0.22	0.15		
72. $C_5H_5 + O_2 \rightleftharpoons CH_2CHCHCO + HCO$		−0.04	0.52	0.36	0.01	−0.05	0.47	0.09
143. $CH_2CHCHCO + H \rightleftharpoons CH_2CHC.H_2 + CO$			−0.05	−0.02			−0.02	
146. $CH_2CHCHCO + O \rightleftharpoons CH_2HCO + HCCO$			0.03	0.03	0.13	0.09	0.03	0.08
$O + OH \rightleftharpoons H + O_2$		0.10	0.84	0.41	10.59	4.39	0.36	0.62
$OH + H_2 \rightleftharpoons H_2O + H$			0.04	0.15		0.04	0.15	
$2OH \rightleftharpoons O + H_2O$			0.14	0.36	0.93	2.15	0.33	0.22
$H + O_2 + M \rightleftharpoons HO_2 + M$			0.04	0.05	−10.26	−4.27	0.07	−0.07
$H + HO_2 \rightleftharpoons OH + OH$					0.09	0.08		
$O + HO_2 \rightleftharpoons O_2 + OH$			−0.01		−0.06	−0.05		
$OH + HO_2 \rightleftharpoons H_2O + O_2$		−0.19	−0.01	−0.02	−0.20	−0.32		−0.01
$HO_2 + HO_2 \rightleftharpoons H_2O_2 + O_2$		0.26			0.26	0.28		
$H_2O_2 + M \rightleftharpoons OH + OH + M$		0.08		0.15	0.17			
$HCO + M \rightleftharpoons H + CO + M$		0.06	−0.02	−0.02	0.95	0.23	−0.03	
$CH_4 + HO_2 \rightleftharpoons CH_3 + H_2O_2$		−0.06	0.02	0.02	−0.95	−0.23		
$NO + O + M \rightleftharpoons NO_2 + M$							−0.03	−0.11
$NO + OH + M \rightleftharpoons HONO + M$								−0.07
$NO + HO_2 \rightleftharpoons NO_2 + OH$								0.10

* The sensitivity coefficients are given as $A_i\delta Y_j/Y_j\delta A_i$, where A_i is the preexponential constant for reaction i and Y_j is the mass fraction of the jth species. Therefore, the sensitivity coefficients listed can be interpreted as the relative change in predicted concentration for the species j caused by increasing the rate constant for reactoin i by a factor of 2.

and, at higher temperatures, also by thermal dissociation:

$$C_6H_5OH \rightleftharpoons C_5H_6 + CO \qquad (20)$$

Subsequently, C_6H_5O and C_5H_6 may be converted to C_5H_5 by CO elimination (15) or H abstraction reactions, respectively. The phenoxy radical may also react with O atoms, forming benzoquinone (17, 18). Under the conditions of Figure 2, pOC_6H_4O is consumed primarily by reaction with the radical pool, while oOC_6H_4O decomposes thermally. Cyclopentadienyl is consumed by reaction with the O/H radical pool or O_2. The calculations are most sensitive to the reactions with HO_2 and O_2 (Table II), forming oxygenated cyclic and linear species:

$$C_5H_5 + HO_2 \rightleftharpoons C_5H_5O + OH \qquad (71)$$

$$C_5H_5 + O_2 \rightleftharpoons CH_2CHCHCO + HCO \qquad (72)$$

A minor consumption pathway occurs through isomerization followed by ring opening:

$$C_5H_5 \rightleftharpoons CHCCHCH\dot{C}H_2 \quad (65)$$

$$CHCCHCH\dot{C}H_2 \rightleftharpoons H_2CCCH + C_2H_2 \quad (112)$$

The cyclic oxygenated compounds are mostly converted by H abstraction/H elimination reactions (C_5H_5OH, C_5H_4OH, and C_5H_5O) or by CO elimination (oOC_6H_4O) to C_5H_4O, which is the most stable of these species. Cyclopentadienone, as well as parabenzoquinone, builds up at lower temperatures; but at higher temperatures, it leads to ring opening, mainly by reaction with the radical pool.

The good agreement between experimental data and modeling predictions for pyrolysis and oxidation of phenol indicate that the overall features of the phenol chemistry are adequately described by the present reaction mechanism. However, a thorough validation of the phenol oxidation subset of the mechanism would require comparison of modeling predictions to a larger and more detailed experimental database. The phenol chemistry is quite complex and the uncertainties related to the reactions by cyclopentadienyl and oxygenated intermediates are significant.

Benzene Oxidation

The oxidation of benzene under flow-reactor conditions was studied over a large range of stoichiometries in the temperature range 900–1400 K. In addition to varying the stoichiometry, the radical pool composition (at a fixed stoichiometry) was perturbed by changing the relative proportion between oxygen and water vapor or by adding NO. The perturbation experiments emphasize particular subsets of the oxidation chemistry and may provide important data for model development and validation.

Figure 3 compares experimental results and model calculations for C_6H_6, CO, and CO_2 as a function of temperature obtained for stoichiometries ranging from stoichiometric ($\lambda = 1.04$) to very lean conditions ($\lambda = 600$). Independent of the stoichiometry, benzene oxidation is initiated at about 1000 K. As the temperature increases, the rate of consumption of benzene depends strongly on the oxygen concentration. At high O_2 levels, benzene is almost completely consumed at 1100 K; but at stoichiometric conditions, this temperature is shifted almost 200 K towards higher temperatures. A similar shift in temperature is observed for the profiles of CO and CO_2. The two high excess-air-ratio experiments provide very similar results. However, although no significant differences are seen for CO and CO_2 among the two low excess-air sets, a significant shift in C_6H_6 profiles is observed.

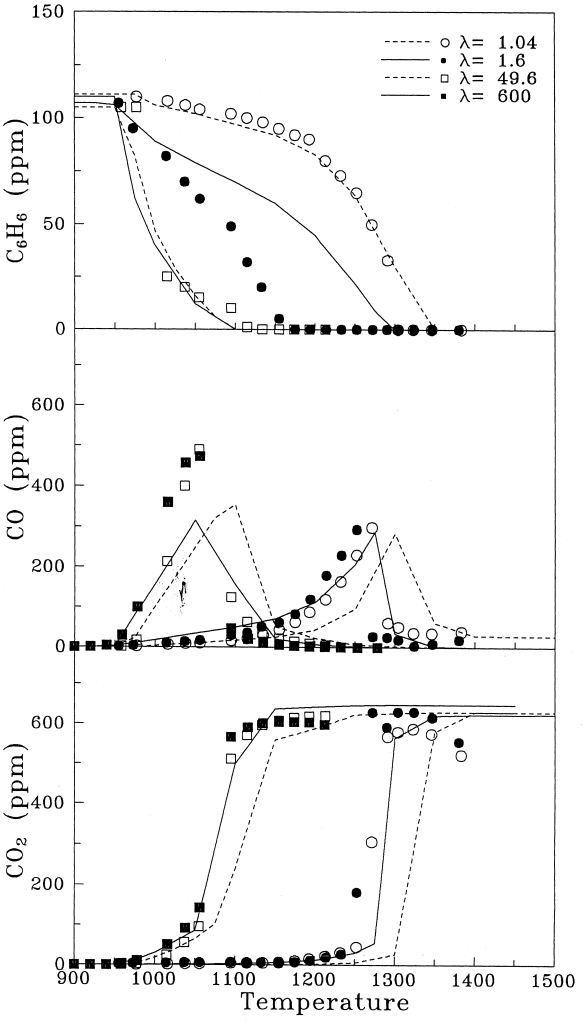

Figure 3 Comparison between experimental data and model predictions for C_6H_6, CO, and CO_2 during the oxidation of benzene for different stoichiometries as a function of temperature. The inlet conditions are listed in Table I ($\lambda = 1.04$, Set 3; $\lambda = 1.6$, Set 5; $\lambda = 49.6$, Set 7; $\lambda = 600$, Set 11).

The model predicts well the experimental trends, both the temperature regime for oxidation and the concentration profiles. However, for the lean conditions and at lower temperatures, a carbon balance indicates that the model underpredicts the conversion of intermediate C_4 and C_5 compounds. In particular, pOC_6H_4O and C_5H_4O appear to be overpredicted; these compounds build up in concentration in the calculations and cause underprediction of CO and CO_2. Furthermore, the C_6H_6 oxidation rate for the $\lambda = 1.6$ set is somewhat underpredicted.

Figure 4 shows a reaction path diagram for the oxidation of benzene, based on rate-of-production analysis of the calculations. The analysis indicates that the major pathways for benzene oxidation (shown as solid lines in the diagram) are similar for the variety of conditions studied in this work. In addition to these reaction paths, a number of minor pathways are active close to stoichiometric conditions; these are shown in Figure 4 as dotted lines.

Benzene oxidation is initiated by reaction with the radical pool, forming phenyl or feeding into the phenol/phenoxy pool:

$$C_6H_6 + OH \rightleftharpoons C_6H_5 + H_2O \qquad (3)$$

$$C_6H_6 + OH \rightleftharpoons C_6H_5OH + H \qquad (-22)$$

$$C_6H_6 + O \rightleftharpoons C_6H_5O + H \qquad (1)$$

Phenyl reacts solely with O_2, forming mainly phenoxy:

$$C_6H_5 + O_2 \rightleftharpoons C_6H_5O + O \qquad (13)$$

but with a significant secondary channel, presumably forming orthobenzoquinone:

$$C_6H_5 + O_2 \rightleftharpoons oOC_6H_4O + H \qquad (14)$$

Most of the phenol is converted to phenoxy through reactions with the radical pool:

$$C_6H_5OH + OH \rightleftharpoons C_6H_5O + H_2O \qquad (24)$$

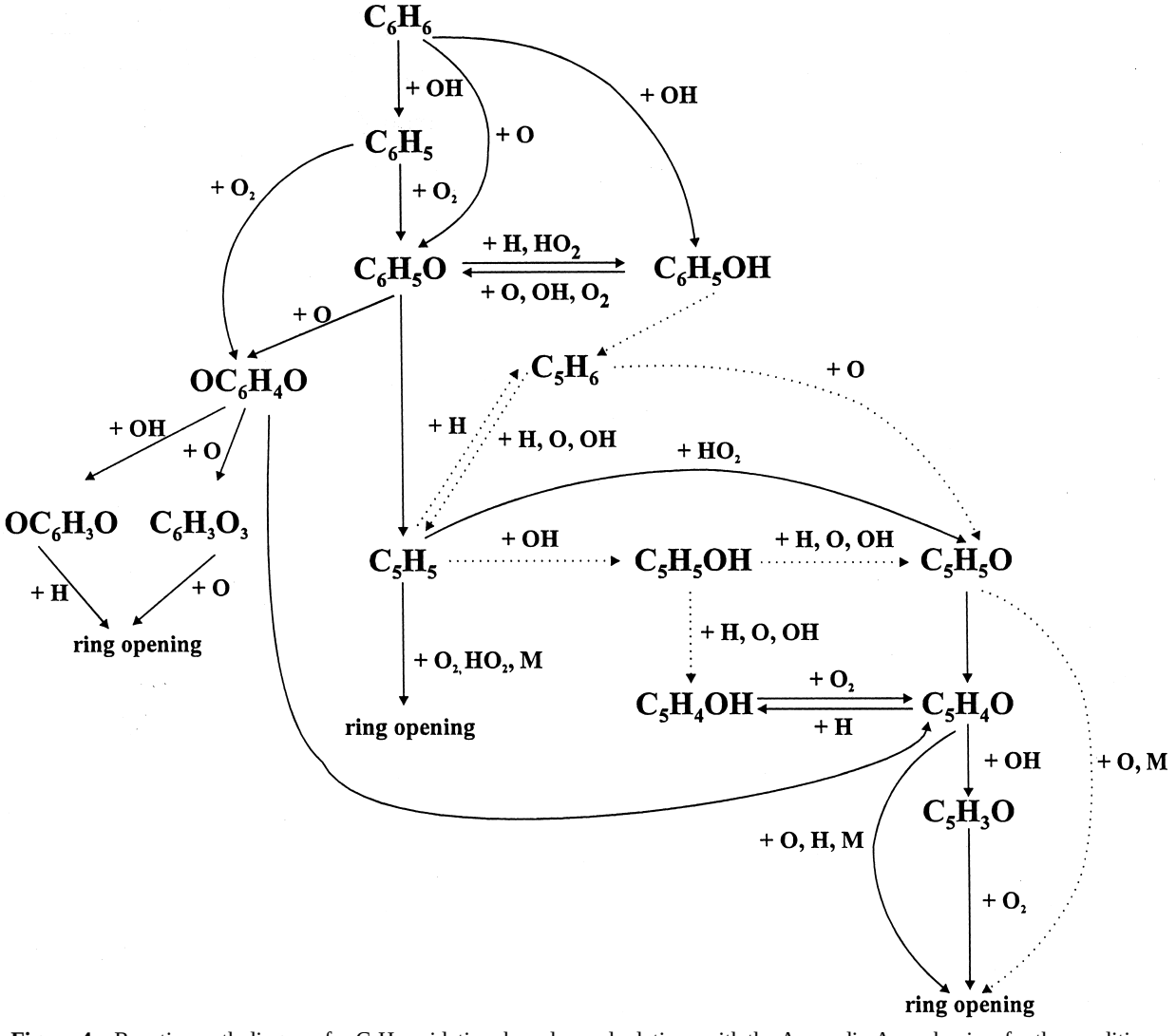

Figure 4 Reaction path diagram for C_6H_6 oxidation, based on calculations with the Appendix A mechanism for the conditions of Figure 3. Solid lines denote the major oxidation pathways; dotted lines denote minor reaction pathways important only under the close-to-stoichiometric conditions.

$$C_6H_5OH + O \rightleftharpoons C_6H_5O + OH \quad (23)$$

$$C_6H_5OH + HO_2 \rightleftharpoons C_6H_5O + H_2O_2 \quad (26)$$

Phenoxy radicals formed in significant quantities from phenyl and phenol thereby become an important link between the aromatic and nonaromatic hydrocarbons during the benzene oxidation process. They are largely converted to cyclopentadienyl radicals and benzoquinone:

$$C_6H_5O \rightleftharpoons C_5H_5 + CO \quad (15)$$

$$C_6H_5O + O \rightleftharpoons OC_6H_4O + H \quad (17, 18)$$

Due to the uncertainties of the reactions $C_6H_5 + O_2$ (14) and $C_6H_5O + O$ (17, 18), the amount of benzoquinone formed and the ratio between the two isomers are quite uncertain. However, our calculations indicate that the model predictions for the overall oxidation behavior of benzene (i.e., the concentrations of C_6H_6, CO, and CO_2) are not very sensitive to these uncertainties in the mechanism. *p*OC_6H_4O is consumed primarily by reaction with the radical pool, presumably leading to ring opening; *o*OC_6H_4O decomposes by CO elimination, forming C_5H_4O. Despite these differences in oxidation pathways, model predictions varying the products (parabenzoquinone or orthobenzoquinone) or the rate (Appendix A value or zero) of reaction (14) provide similar results for C_6H_6, CO, and CO_2. This is consistent with the fact that none of the benzoquinone consumption reactions show up in the sensitivity analysis (Table II).

The cyclopentadienyl radical formed in reaction (15) is a key intermediate in the oxidation process, and modeling predictions are very sensitive to the reactions involving this radical (Table II). The chemistry of cyclopentadienyl is very complicated and has been shown to involve numerous reaction pathways and species [18]. It is worth noticing that the introduction into the mechanism of the C_5H_5 subset from Zhong and Bozzelli [18] significantly improved model predictions for the present conditions.

Under the conditions of this work, C_5H_5 is consumed mostly by reaction with HO_2, forming C_5H_5O:

$$C_5H_5 + HO_2 \rightleftharpoons C_5H_5O + OH \quad (71)$$

or by ring-opening reactions,

$$C_5H_5 + O \rightleftharpoons CH_2CHCH\dot{C}H + CO \quad (67)$$

$$C_5H_5 + O_2 \rightleftharpoons CH_2CHCHCO + HCO \quad (72)$$

$$C_5H_5 \rightleftharpoons CHCCHCH\dot{C}H_2 \quad (65)$$

Under close to stoichiometric conditions, recombination reactions with H and OH radicals become important:

$$C_5H_5 + H \rightleftharpoons C_5H_6 \quad (66)$$

$$C_5H_5 + OH \rightleftharpoons C_5H_5OH \quad (69)$$

The reaction sequence, involving reaction (66) followed by recycling of cyclopentadiene to cyclopentadienyl by reaction with the radical pool (49, 53, 55), constitutes an important chain-terminating process. The fate of C_5H_5OH and the derived radicals, C_5H_5O and C_5H_4OH, is not well established. Following Zhong and Bozzelli [35], we assume C_5H_5OH to be consumed by abstraction reactions:

$$C_5H_5OH + H, O, OH \rightleftharpoons C_5H_5O/C_5H_4OH + H_2, OH, H_2O \quad (75-80)$$

The C_5H_5O and C_5H_4OH radicals are largely converted to C_5H_4O by thermal decomposition or reaction with O_2:

$$C_5H_5O \rightleftharpoons C_5H_4O + H \quad (73)$$

$$C_5H_4OH \rightleftharpoons C_5H_4O + H \quad (92)$$

$$C_5H_4OH + O_2 \rightleftharpoons C_5H_4O + HO_2 \quad (94)$$

with a smaller fraction of C_5H_5O eliminating CO and leading to ring opening:

$$C_5H_5O \rightleftharpoons CH_2CHCH\dot{C}H + CO \quad (74)$$

According to the mechanism, cyclopentadienone is consumed mainly by reaction with the radical pool,

$$C_5H_4O + OH \rightleftharpoons C_5H_3O + H_2O \quad (91)$$

$$C_5H_4O + H \rightleftharpoons C_2CHCH\dot{C}H + CO \quad (87)$$

$$C_5H_4O + O \rightleftharpoons C_2CHCCH + CO_2 \quad (89)$$

while thermal dissociation (86) is less important under these conditions. In the modeling, cyclopentadienone is the most stable of these oxygenated cyclic compounds. However, as discussed earlier, there are experimental indications that significant consumption steps for this component are missing from the mechanism.

The first-order sensitivity coefficients for CO listed in Table II correspond to the initiation conditions of selected benzene oxidation experiments. The results indicate that the oxidation of benzene is mainly sensitive to the C_6-C_5 reaction subset. Apart from the initiation reactions of benzene, the calculations are

sensitive to reactions involving C_6H_5, C_6H_5O, and C_6H_5OH and to the fate of the cyclopentadienyl radical. However, the sensitivity analysis should be interpreted very cautiously due to the large uncertainties in the reaction mechanism. As long as even the major oxidation route for benzene oxidation is in question, a sensitivity analysis may provide misleading results.

In order to further investigate the oxidation characteristics of benzene, we perturbed the radical pool in the experiments by varying the amount of H_2O and by adding NO. Figure 5 compares experimental and calculated results for water vapor levels of 0.5 and 4.8%, respectively, for very lean conditions.

The water vapor level affects the composition of the radical pool mainly by its influence on the OH/O ratio. Under lean conditions, the presence of water vapor acts to convert one O radical into two hydroxyl radicals through the fast shuffle reaction:

$$O + H_2O \rightleftharpoons OH + OH$$

This step shifts the OH/O ratio to higher values. The effect is difficult to quantify, because it depends on reactant composition, temperature, and oxidation rate; but for the lean conditions, the OH/O ratio is generally increased by a factor of 2–5 by increasing the H_2O level from 0.5 to 5%. In high concentrations, water may also affect the composition of the radical pool by acting as an efficient collision partner in the reaction:

$$H + O_2 + M \rightleftharpoons HO_2 + M$$

converting the highly reactive H atom into the comparatively unreactive HO_2 radical.

The results of Figure 5 show that even under very lean conditions, where the effect would be expected to be most pronounced, the impact of the water vapor level is only minor and within the experimental uncertainty. A small shift in the temperature for onset of oxidation of benzene is observed, but the CO and CO_2 profiles are largely unchanged. The model correctly predicts the small shift in the benzene concentration profile but overestimates the effect of the increased OH/O ratio at the higher H_2O level on the oxidation of CO to CO_2.

The influence of NO addition on oxidation of benzene is shown in Figure 6, which compares results obtained in the absence and in the presence of 100 ppm NO as a function of temperature for stoichiometric and very lean conditions. The presence of NO changes the composition of the radical pool through the reaction

$$NO + HO_2 \rightleftharpoons NO_2 + OH$$

This step converts the unreactive HO_2 radical into OH. Thereby, the presence of NO may significantly promote fuel oxidation under lean conditions in the 900–1200 K range [66,67]. Subsequently, NO_2 is partially recycled to NO by reaction with O or H atoms [66,67]. Under stoichiometric or fuel-rich conditions the concentration of the HO_2 radical is smaller and the promoting effect of NO by this mechanism diminishes. The presence of NO may also promote oxidation by direct interaction with the fuel oxidation chemistry [68,69]. Such an interaction is not believed to be significant under the present conditions, even though some reaction between benzene-derived radicals and NO is likely to occur.

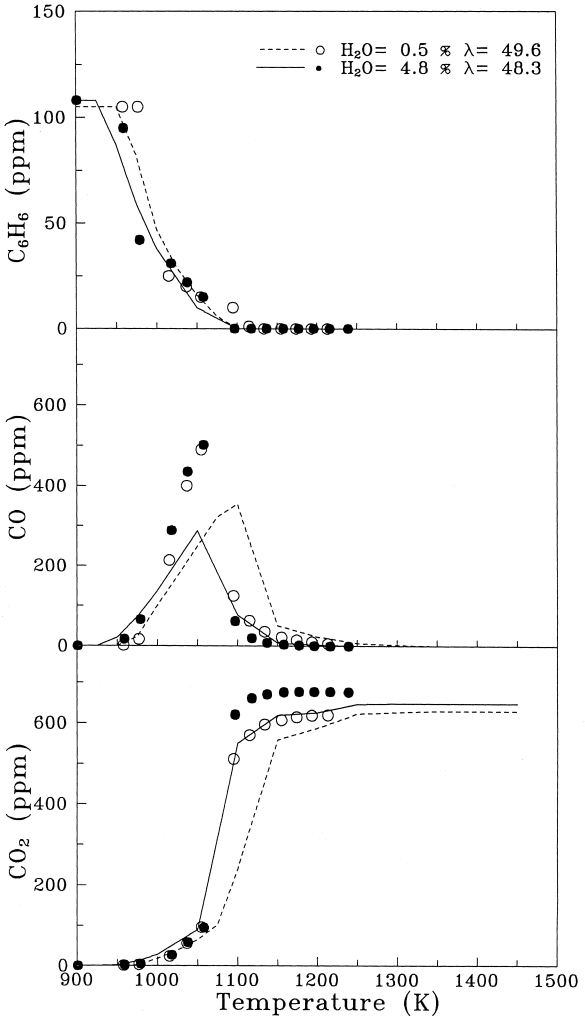

Figure 5 Comparison between experimental data and model predictions for C_6H_6, CO, and CO_2 profiles during the oxidation of benzene for different stoichiometries and water vapor levels as function of temperature. The inlet conditions are listed in Table I (λ = 49.6 and 0.5% H_2O: Set 7; λ = 48.3 and 4.8% H_2O; Set 9).

Figure 6 shows that under very lean conditions the presence of NO shifts the oxidation regime of C_6H_6 and the formation of CO and CO_2 towards lower temperatures (~60–80 K). Between 900 and 1000 K, a significant fraction, 10–30%, of the inlet NO is emitted as NO_2. At excess-air ratios close to stoichiometric, no sensitization of the C_6H_6 oxidation by NO is seen and very little NO_2 is predicted. Under these conditions, presence of NO causes a slight inhibition of the oxidation, due to NO-catalyzed recombination of radicals [67].

The modeling predictions are in reasonably good agreement with the experimental observations. The model predicts correctly the shift in the temperature for onset of oxidation caused by the NO under lean conditions as well as the slight inhibition observed for $\lambda = 1.6$. Compared to other fuels [66–69], the promoting effect of NO under lean conditions is fairly small for benzene. This indicates that other pseudo-chain-branching steps involving HO_2 compete with the $NO + HO_2$ reaction. Apart from the reaction with NO, HO_2 is primarily removed through the following reactions:

$$C_6H_5O + HO_2 \rightleftharpoons C_6H_5OH + O_2 \quad (-25)$$

$$C_6H_5OH + HO_2 \rightleftharpoons C_6H_5O + H_2O_2 \quad (26)$$

$$C_5H_5 + HO_2 \rightleftharpoons C_5H_5O + OH \quad (71)$$

$$C_5H_5 + HO_2 \rightleftharpoons C_5H_6 + O_2 \quad (-58)$$

Of these reactions, only reaction (71), which produces C_5H_5O and OH radicals, is chain propagating; the other reactions are chain terminating. However, they all contribute to remove HO_2 and thereby minimize the influence of the $NO + HO_2$ reaction.

In summary, the results of Figures 5 and 6 indicate that the oxidation rate of benzene under the conditions investigated is mainly controlled by the stoichiometry and the temperature. The radical pool composition, specifically the O/OH ratio and the HO_2 level, is comparatively less important.

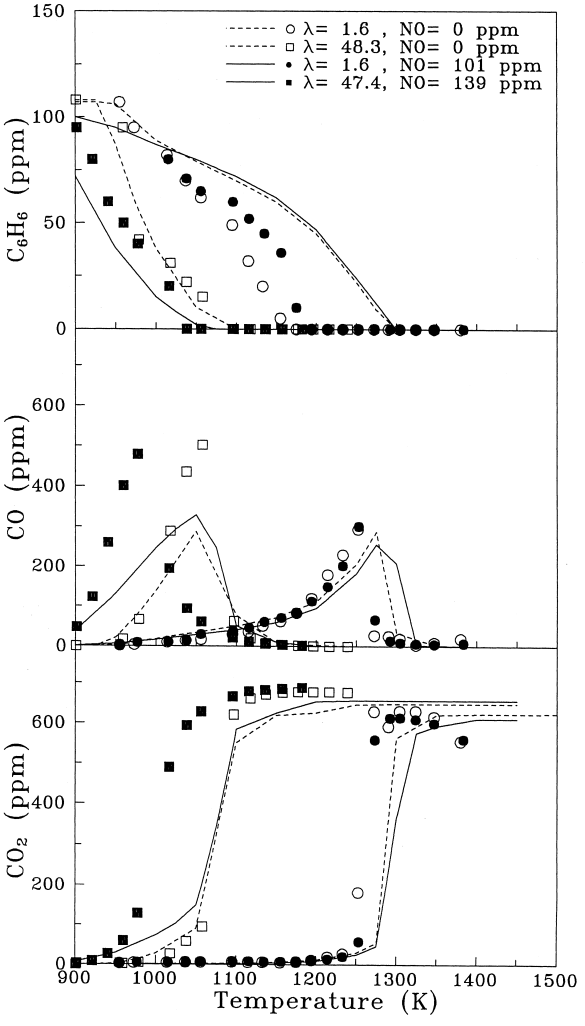

Figure 6 Comparison between experimental data and model predictions for C_6H_6, CO, and CO_2 during the oxidation of benzene for different stoichiometries and NO levels as function of temperature. The inlet conditions are listed in Table I ($\lambda = 1.04$ and 0 ppm NO: Set 3; $\lambda = 48.3$ and 0 ppm NO: Set 9; $\lambda = 1.6$ and 100 ppm NO: Set 4; $\lambda = 47.4$ and 100 ppm NO: Set 10).

The Flow Reactor Data of Lovell et al. The experimental results of Lovell et al. [6] on lean benzene oxidation were used to further evaluate the benzene oxidation scheme. These data were obtained in a turbulent flow reactor under near-adiabatic conditions. The concentrations of C_6H_6, C_6H_5OH, C_5H_6, C_4/C_2 hydrocarbons, and CO were measured as function of axial distance in the reactor. Due to some uncertainty in the velocity profile for the experiments [9], the reaction time is only accurate within 15–20%.

The initial mixing of reactants in the reactor is known to affect the chemical induction time. For this reason, modeling results are shifted in time to match the measured benzene level at the point of the highest concentration gradient. This approach has been shown to be valid, since the induction chemistry has only a negligible effect on the postinduction species profiles [9].

Figure 7 compares experimental results [6] and model predictions for lean benzene oxidation at 1100 K. The overall agreement is reasonable, considering the uncertainties in the mechanism just discussed. The predicted benzene consumption rate is slightly lower than observed; this discrepancy affects also the pre-

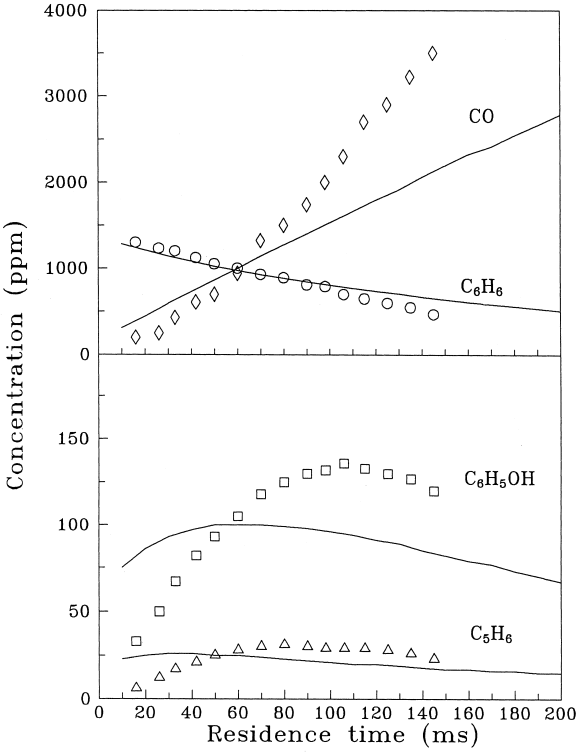

Figure 7 Comparison between experimental data [6] and model predictions for oxidation of benzene in an adiabatic flow reactor. Inlet composition is C_6H_6 = 1571 ppm, O_2 = 15,900 ppm; balance N_2. Inlet temperature is 1098 K, atmospheric pressure.

dictions for C_6H_5OH, C_5H_6, and CO. However, the peak levels of C_6H_5OH and C_5H_6 are fairly well predicted. At longer reaction times, CO is significantly underpredicted; this can be attributed mostly to buildup of cyclic intermediates such as *p*OC_6H_4O and C_5H_4O in the calculations.

The Stirred Reactor Data of Chai and Pfefferle. Even at comparable temperatures, experimental conditions in a jet-stirred reactor are quite different from those of a flow reactor. For this reason, we wished to supplement the flow-reactor data from the present study and those of Lovell et al. with the well-mixed-reactor results reported by Chai and Pfefferle [19]. Chai and Pfefferle performed their experiments in a micro-jet reactor, which approaches a well-stirred reactor under the conditions investigated. Their experiments, which covered the temperature range 900–1300 K, were performed at nominal residence times of ~50 ms and pressures of 350 torr. The products of reaction were measured by a residual gas analyzer and time-of-flight mass spectrometers. Thereby, a very detailed characterization of the product composition was feasible.

Figure 8 compares experimental results reported by Chai and Pfefferle [19] for lean benzene oxidation with model predictions. Benzene oxidation is initiated at ~1000 K, and benzene is largely depleted at 1100 K. The major intermediates are C_2H_2 and CO, which reach peak values of 1000 and 10,000 ppm, respectively. Apart from benzene, phenol is the most abundant aromatic compound (around 40 ppm). From the figure, it is evident that the model overpredicts the benzene oxidation rate, shifting the temperature for complete consumption of C_6H_6 almost 50 K to lower temperatures. However, the modeling results must be interpreted with some caution due to the occurrence of multiple solutions. The solution shown is the one with the greatest extent of reaction.

The most remarkable discrepancies between experimental data and modeling predictions concern phenol and benzoquinone (shown in Fig. 8) as well as cyclopentadienone and acetylene (not shown). The present mechanism grossly overpredicts the concentration of the cyclic intermediates C_6H_5OH, OC_6H_4O, and C_5H_4O (note the logarithmic scale used for the bottom part of Fig. 8). Correspondingly, the levels of C_2H_2

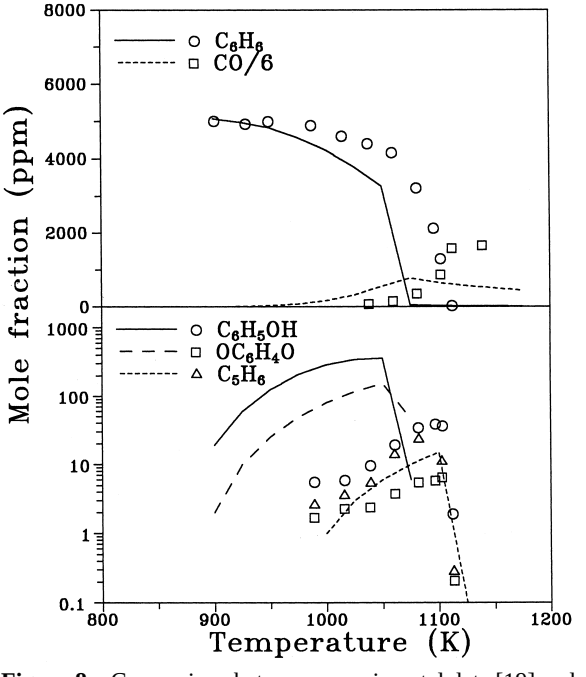

Figure 8 Comparison between experimental data [19] and model predictions for oxidation of benzene in a jet-stirred reactor. Inlet composition is C_6H_6 = 5100 ppm, O_2 = 2.0% (vol); balance Ar. Pressure is 0.46 atm; nominal residence time is 50 ms.

Appendix A The C_3–C_6 Reaction Subset in the Benzene Oxidation Mechanism

		A	β	E_a	Source
	Cyclic C_6 species				
1.	$C_6H_6 + O \rightleftharpoons C_6H_5O + H$	2.2E13	0.00	4530	[26, 39]
2.	$C_6H_6 + O \rightleftharpoons C_6H_5O + OH$	2.0E13	0.00	14,700	[40]
3.	$C_6H_6 + OH \rightleftharpoons C_6H_5 + H_2O$	1.6E08	1.42	1450	[25]
4.	$C_6H_6 + O_2 \rightleftharpoons C_6H_5 + HO_2$	6.0E13	0.00	63,400	est
5.	$C_6H_5 \rightleftharpoons C_6H_4 + H$	1.4E15	0.00	83,860	[21], est
6.	$C_6H_5 + H \rightleftharpoons C_6H_6$	2.0E14	0.00	0	[21, 70]
7.	$C_6H_5 + H \rightleftharpoons C_6H_4 + H_2$	2.0E07	2.00	1000	[27] est
8.	$C_6H_5 + O \rightleftharpoons C_5H_5 + CO$	1.0E14	0.00	0	[20]
9.	$C_6H_5 + OH \rightleftharpoons C_6H_6O + H$	5.0E13	0.00	0	[27] est
10.	$C_6H_5 + OH \rightleftharpoons C_6H_4 + H_2O$	1.0E07	2.00	1000	[27] est
11.	$C_6H_5 + HO_2 \rightleftharpoons C_6H_5O + OH$	3.0E13	0.00	0	est
12.	$C_6H_5 + H_2 \rightleftharpoons C_6H_6 + H$	5.7E04	2.43	6280	[37]
13.	$C_6H_5 + O_2 \rightleftharpoons C_6H_5O + O$	2.6E13	0.00	6100	[20]
14.	$C_6H_5 + O_2 \rightleftharpoons o\text{-}OC_6H_4O + H$	3.0E13	0.00	9000	[20], see text
15.	$C_6H_5O \rightleftharpoons C_5H_5 + CO$	7.4E11	0.00	43,900	[20]
16.	$C_6H_5O + H \rightleftharpoons C_6H_5OH$	2.5E14	0.00	0	[25]
17.	$C_6H_5O + O \rightleftharpoons p\text{-}OC_6H_4O + H$	8.5E13	0.00	0	[51], est
18.	$C_6H_5O + O \rightleftharpoons o\text{-}OC_6H_4O + H$	8.5E13	0.00	0	[51], est
19.	$C_6H_5O + O \rightleftharpoons C_5H_5 + CO_2$	1.0E13	0.00	0	[51]
20.	$C_6H_5OH \rightleftharpoons C_5H_6O + CO$	1.0E12	0.00	60,800	[48]
21.	$C_6H_5OH + H \rightleftharpoons C_6H_5O + H_2$	1.2E14	0.00	12,400	[25]
22.	$C_6H_5OH + H \rightleftharpoons C_6H_6 + OH$	2.2E13	0.00	7930	[25]
23.	$C_6H_5OH + O \rightleftharpoons C_6H_5O + OH$	1.3E13	0.00	2900	[26]
24.	$C_6H_5OH + OH \rightleftharpoons C_6H_5O + H_2O$	3.0E06	2.00	−1310	[47]
25.	$C_6H_5OH + O_2 \rightleftharpoons C_6H_5O + HO_2$	1.0E13	0.00	38,000	est
26.	$C_6H_5OH + HO_2 \rightleftharpoons C_6H_5O + H_2O_2$	1.0E12	0.00	1000	est
27.	$C_6H_5OH + C_2H_3 \rightleftharpoons \dot{C}_6H_5O + C_2H_4$	6.0E12	0.00	0	[9] est
28.	$C_6H_5OH + CH_2C\dot{C}CH_2 \rightleftharpoons C_6H_5O + CH_2CHCHCH_2$	6.0E12	0.00	0	[9] est
29.	$C_6H_5OH + C_6H_5 \rightleftharpoons C_6H_5O + C_6H_6$	4.9E12	0.00	4400	[71]
30.	$o\text{-}OC_6H_4O \rightleftharpoons C_5H_4O + CO$	1.0E12	0.00	40,000	est
31.	$p\text{-}OC_6H_4O \rightleftharpoons C_5H_4O + CO$	3.7E11	0.00	59,000	[22]
32.	$p\text{-}OC_6H_4O \rightleftharpoons C_5H_4 + CO_2$	3.5E12	0.00	67,000	[22]
33.	$p\text{-}OC_6H_4O + H \rightleftharpoons C_5H_5O$[a] $+ CO$	2.5E13	0.00	4700	[22] est
34.	$p\text{-}OC_6H_4O + H \rightarrow OC_6H_3O + H_2$	2.0E12	0.00	8100	[22] est[b]
35.	$p\text{-}OC_6H_4O + O \rightarrow C_6H_3O_3 + H$	1.5E13	0.00	4530	[22] est[b]
36.	$p\text{-}OC_6H_4O + O \rightleftharpoons OC_6H_3O + OH$	1.4E13	0.00	14,700	[22] est[b]
37.	$p\text{-}OC_6H_4O + OH \rightleftharpoons OC_6H_3O + H_2O$	1.0E06	2.00	4000	[22]
38.	$OC_6H_3O + H \rightarrow p\text{-}OC_6H_4O + OH$	1.0E14	0.00	0	est
39.	$OC_6H_3O + H \rightarrow 2C_2H_2 + 2CO$	1.0E14	0.00	0	[22] est
40.	$OC_6H_3O + O \rightarrow C_2H_2 + HCCO + 2CO$	1.0E14	0.00	0	[22] est
41.	$C_6H_3O_3 \rightarrow C_2H_2 + HCCO + 2CO$	1.0E12	0.00	50,000	[22] est
42.	$C_6H_3O_3 + H \rightarrow C_2H_2 + CH_2CO + 2CO$	1.0E14	0.00	0	est
	Cyclic C_5 species				
43.	C_5H_7[a] $\rightleftharpoons CH_2C\dot{H}CHCHCH_2$	3.2E15	0.00	39,500	[72]
44.	$C_5H_7 + H \rightleftharpoons C_5H_6 + H_2$	3.6E12	0.00	0	est[c]
45.	$C_5H_7 + O \rightleftharpoons C_5H_6 + OH$	1.0E13	0.00	0	est
46.	$C_5H_7 + OH \rightleftharpoons C_5H_6 + H_2O$	2.4E13	0.00	0	[35] est[c]
47.	$C_5H_7 + O_2 \rightleftharpoons C_5H_6 + HO_2$	1.3E11	0.00	0	est[c]
48.	$C_5H_7 + O_2 \rightleftharpoons CHOCH_2CH_2\dot{C}HCHCO$	8.0E24	−3.80	20,000	[35] qrrk
49.	$C_5H_6 + H \rightleftharpoons C_5H_5 + H_2$	7.2E13	0.00	3500	[56]
50.	$C_5H_6 + H \rightleftharpoons \dot{C}_5H_7$	2.4E73	−17.85	31,500	[18] qrrk
51.	$C_5H_6 + H \rightleftharpoons CH_2C\dot{C}HCHCH_2$	1.1E14	−0.16	3100	[18] qrrk
52.	$C_5H_6 + O \rightleftharpoons C_5H_5O + H$	8.9E12	−0.15	590	[18] qrrk
	$C_5H_6 + O \rightleftharpoons C_5H_5O + H$	5.6E12	−.06	200	[18] qrrk

(Continued)

Appendix A (Continued)

		A	β	E_a	Source
	Duplicate reaction[a]				
53.	$C_5H_6 + O \rightleftharpoons C_5H_5 + OH$	4.8E04	2.71	1100	[18] est[c]
54.	$C_5H_6 + OH \rightleftharpoons CH_2CH\dot{C}HCHCHOH$	1.1E13	−0.07	870	[18] qrrk
55.	$C_5H_6 + OH \rightleftharpoons C_5H_5 + H_2O$	3.1E06	2.00	0	[18] est[d]
56.	$C_5H_6 + HO_2 \rightleftharpoons C_5H_7 + O_2$	1.3E15	−1.07	9530	[18] qrrk
57.	$C_5H_6 + HO_2 \rightleftharpoons C_5H_5 + O_2$	1.1E04	2.60	12,900	[18] est[c]
58.	$C_5H_6 + O_2 \rightleftharpoons C_5H_5 + HO_2$	4.0E13	0.00	37,150	[18] est[c]
59.	$C_5H_6 + CH_3 \rightleftharpoons C_5H_5 + CH_4$	1.8E-1	4.00	0	[18] est[c]
60.	$C_5H_6 + C_2H_3 \rightleftharpoons C_6H_6 + CH_3$	2.1E67	−16.08	42,460	[18] est[c]
61.	$C_5H_6 + C_2H_3 \rightleftharpoons C_5H_5 + C_2H_4$	1.2E-1	4.00	0	[18] est[c]
62.	$C_5H_6 + C_6H_5 \rightleftharpoons C_6H_6 + C_5H_5$	1.0E-1	4.00	0	[18] est[c]
63.	$C_5H_6 + CH_2CH\dot{C}C\dot{C}H_2 \rightleftharpoons C_5H_5 + CH_2CHCHCH_2$	6.0E12	0.00	0	[9] est
64.	$C_5H_6 + C_6H_5O \rightleftharpoons C_5H_5 + C_6H_5OH$	3.2E11	0.00	8000	[9] est
65.	$C_5H_5 \rightleftharpoons CHCCHCHCH_2$	1.0E12	1.00	77,000	[56]
66.	$C_5H_5 + H \rightleftharpoons C_5H_6$	1.5E14	0.00	0	[21, 59]
67.	$C_5H_5 + O \rightleftharpoons CH_2CHCH\dot{C}H + CO$	3.2E13	−0.17	440	[18] qrrk
68.	$C_5H_5 + O \rightleftharpoons C_5H_4O + H$	5.8E13	−0.02	20	[18] qrrk
69.	$C_5H_5 + OH \rightleftharpoons C_5H_5OH$	6.5E14	−0.85	−2730	[18] qrrk
	$C_5H_5 + OH \rightleftharpoons C_5H_5OH$	1.1E43	−8.76	18,730	[18] qrrk
	$C_5H_5 + OH \rightleftharpoons C_5H_5OH$	1.1E59	−13.08	33,450	[18] qrrk
	Duplicate reaction[a]				
70.	$C_5H_5 + OH \rightleftharpoons C_5H_4OH + H$	3.5E57	−12.18	48,350	[18] qrrk
71.	$C_5H_5 + HO_2 \rightleftharpoons C_5H_5O + OH$	6.3E29	−4.69	11,650	[18] qrrk
72.	$C_5H_5 + O_2 \rightleftharpoons CH_2CHCHCO + HCO$	1.2E19	−2.48	10,970	[18] qrrk
73.	$C_5H_5O \rightleftharpoons C_5H_4O + H$	2.9E32	−6.50	21,220	[35] qrrk
74.	$C_5H_5O \rightleftharpoons CH_2CHCH\dot{C}H + CO$	1.1E79	−19.62	66,250	[35] qrrk
75.	$C_5H_5OH + H \rightleftharpoons C_5H_4OH + H_2$	3.2E12	0.00	0	[35] est[c]
76.	$C_5H_5OH + H \rightleftharpoons C_5H_5O + H_2$	4.0E13	0.00	6094	[35] est[d]
77.	$C_5H_5OH + O \rightleftharpoons C_5H_4OH + OH$	4.7E11	0.00	0	[35] est[d]
78.	$C_5H_5OH + O \rightleftharpoons C_5H_5O + OH$	1.0E13	0.00	4683	[35] est[d]
79.	$C_5H_5OH + OH \rightleftharpoons C_5H_4OH + H_2O$	5.5E12	0.00	1731	[35] est[d]
80.	$C_5H_5OH + OH \rightleftharpoons C_5H_5O + H_2O$	1.0E13	0.00	1697	[35] est[d]
81.	$C_5H_5OH + HO_2 \rightleftharpoons C_5H_4OH + H_2O_2$	3.6E03	2.55	10,531	[35] est
82.	$C_5H_5OH + HO_2 \rightleftharpoons C_5H_5O + H_2O_2$	1.0E13	0.00	15,800	[35] est
83.	$C_5H_4 + H \rightleftharpoons C_5H_3 + H_2$	1.0E06	2.50	5000	[22] est
84.	$C_5H_4 + O \rightleftharpoons C_5H_3 + H_2$	1.0E06	2.50	3000	[22] est
85.	$C_5H_4 + OH \rightleftharpoons C_5H_3 + H_2O$	1.0E06	2.00	0	[22] est
86.	$C_5H_4O \rightarrow C_2H_2 + C_2H_2 + CO$	5.7E32	−6.76	68,500	[23][e]
	$C_5H_4O \rightarrow C_2H_2 + C_2H_2 + CO$	6.2E41	−7.87	98,700	
	Duplicate reaction				
87.	$C_5H_4O + H \rightleftharpoons CH_2CHCH\dot{C}H + CO$	2.1E61	−13.27	40,810	[35] qrrk
88.	$C_5H_4O + H \rightleftharpoons C_5H_3O + H_2$	2.0E12	0.00	8100	est[b]
89.	$C_5H_4O + O \rightleftharpoons CH_2CHCCH + CO_2$	1.0E13	0.00	2000	[22] est
90.	$C_5H_4O + O \rightleftharpoons C_5H_3O + OH$	1.4E13	0.00	14,700	est[b]
91.	$C_5H_4O + OH \rightleftharpoons C_5H_3O + H_2O$	1.1E08	1.42	1450	est[b]
92.	$C_5H_4OH + H \rightleftharpoons C_5H_4O + H$	2.1E13	0.00	54,000	[9], adj[f]
93.	$C_5H_4OH + H \rightleftharpoons C_5H_5OH$	1.0E14	0.00	0	est
94.	$C_5H_4OH + O_2 \rightleftharpoons C_5H_4O + HO_2$	3.0E13	0.00	5000	est
95.	$C_5H_3O + H \rightleftharpoons C_5H_4O$	1.0E14	0.00	0	est
96.	$C_5H_3O + O_2 \rightleftharpoons \dot{C}HCHCHCO + CO_2$	9.7E58	−13.47	38,180	[35] qrrk
97.	$C_5H_3 + H \rightleftharpoons C_5H_4$	1.0E14	0.00	0	est
98.	$C_5H_3 + O_2 \rightleftharpoons C_2H_2 + HCCO + CO$	1.0E12	0.00	0	[22] est

(Continued)

Appendix A (Continued)

		A	β	E_a	Source
	Linear C_5 species				
99.	$CH_2CHCHCHCH_3 + H \rightleftharpoons CH_2CHCHCH_2 + CH_3$	5.2E71	−16.38	51,000	[35] qrrk
100.	$CH_2CHCHCHCH_3 + H \rightleftharpoons CH_2CHCHCHCH_2 + H_2$	7.0E06	2.00	5000	[28] est[c]
101.	$CH_2CHCHCHCH_3 + OH \rightleftharpoons CH_2CHCHCHCH_2 + H_2O$	7.0E06	2.00	0	[28] est[c]
102.	$CH_2CHCHCHCH_2 \rightleftharpoons CH_2CHCHCHCH_2$	5.4E11	−0.70	60	[35]
103.	$CH_2CHCHCHCH_2 + O_2 \rightleftharpoons CH_2CHCHO + CH_2HCO$	1.2E36	−7.25	33,600	[35] qrrk
104.	$CH_2CHCHCHCH_2 + H \rightleftharpoons CH_2CHCHCHCH_3$	2.3E20	−1.60	3020	[35] qrrk
105.	$CH_2CHCHCHCH_2 + H \rightleftharpoons CH_2CHCHCH + CH_3$	2.9E26	−2.18	36,770	[35] qrrk
106.	$CH_2CHCHCHCH_2 + O \rightleftharpoons CH_2CHCHO + C_2H_3$	2.0E14	0.00	0	[28] est[c]
107.	$CH_2CHCHCHCH_2 + OH \rightleftharpoons CH_2CHCHCHCH_2OH$	1.5E13	0.00	0	[35] est[c]
108.	$CH_2CHCHCHCH_2 + O_2 \rightleftharpoons CH_2CHCHCHCHO + CH_2O$	8.2E10	0.18	9140	[35] qrrk
109.	$CH_2CHCHCHCH_2OH + H \rightleftharpoons CH_2CHCHCH_2 + CH_2OH$	2.5E34	−6.12	16,250	[35] qrrk
110.	$CHOCH_2CH_2CHCHO + O_2 \rightleftharpoons CHOCH_2CH_2CHO + HCOO$	6.3E05	1.65	17,480	[35] est
111.	$CH_2CHCHCHCHOH + O_2 \rightleftharpoons CHOCHCHOH + CH_2HCO$	1.2E36	−7.25	33,600	[35] est
112.	$CHCCHCHCH_2 \rightleftharpoons H_2CCCH + C_2H_2$	1.0E12	1.00	31,000	[56]
	C_4 hydrocarbon oxidation subset				
113.	$CH_2CHCHCH_2 + H \rightleftharpoons CH_2CHCHCH + H_2$	3.0E07	2.00	13,000	[27]
114.	$CH_2CHCHCH_2 + H \rightleftharpoons CH_2CHCCH_2 + H_2$	3.0E07	2.00	6000	[27]
115.	$CH_2CHCHCH_2 + O \rightleftharpoons CH_2CHCH_2 + HCO$	6.0E08	1.45	−858	[28]
116.	$CH_2CHCHCH_2 + CH_2HCO + C_2H_3$	1.0E12	0.00	0	[28]
117.	$CH_2CHCHCH_2 + OH \rightleftharpoons CH_2CHCHCH + H_2O$	2.0E07	2.00	5000	[27]
118.	$CH_2CHCHCH_2 + OH \rightleftharpoons CH_2CHCCH_2 + H_2O$	2.0E07	2.00	2000	[27]
119.	$CH_2CHCHCH_2 + O_2 \rightleftharpoons CH_2CHCHCH + HO_2$	3.0E13	0.00	57,800	est
120.	$CH_2CHCHCH_2 + O_2 \rightleftharpoons CH_2CHCCH_2 + HO_2$	3.0E13	0.00	45,850	est
121.	$CHOCH_2CH_2CHO + H \rightleftharpoons CHOCH_2CH_2CO + H_2$	2.3E10	1.05	3279	[35] est[g]
122.	$CHOCH_2CH_2CHO + OH \rightleftharpoons CHOCH_2CH_2CO + H_2O$	3.5E09	1.18	−447	[35] est[g]
123.	$CH_2CHCHCH(+M) = CH_2CHCCH + H(+M)$	1.0E14	0.00	37,000	[27]
	Low pressure limit:	1.0E14	0.00	30,000	
	Enhanced third-body efficiencies:				
	$H_2O = 5$				
124.	$CH_2CHCHCH + H \rightleftharpoons CH_2CHCCH_2 + H$	1.0E14	0.00	0	[27]
125.	$CH_2CHCHCH + H \rightleftharpoons CH_2CHCCH + H_2$	3.0E07	2.00	1000	[27]
126.	$CH_2CHCHCH + OH \rightleftharpoons CH_2CHCCH + H_2O$	2.0E07	2.00	1000	[27]
127.	$CH_2CHCHCH + O_2 \rightleftharpoons CHCHCHO + CH_2O$	1.0E12	0.00	0	[28]
128.	$CH_2CHCHCH + O_2 \rightarrow CH_2CHCCH + HO_2$	1.0E07	2.00	10,000	[28]
129.	$CH_2CHCCH_2(+M) = CH_2CHCCH + H(+M)$	1.0E14	0.00	50,000	[27]
	Low pressure limit:	2.0E15	0.00	42,000	
	Enhanced third-body efficiencies:				
	$H_2O = 5$				
130.	$CH_2CHCCH_2 + H \rightleftharpoons H_2CCCH + CH_3$	1.0E14	0.00	0	[27]
131.	$CH_2CHCCH_2 + OH \rightleftharpoons CH_2CHCCH + H_2O$	3.0E13	0.00	0	[27]
132.	$CH_2CHCHCHO \rightarrow CH_2CHCH_2 + CO$	6.1E05	0.92	−1120	est[h]
133.	$CH_2CHCHCHO + O_2 \rightarrow CH_2CHCHO + HCOO$	1.2E36	−7.25	33,600	est k_{98}
134.	$CHOCH_2CH_2CO + O_2 \rightleftharpoons C_2H_4 + O_2CCHOO$	1.6E45	−9.92	20,670	[35] qrrk
135.	$CH_2CHCCH + H \rightleftharpoons HCCHCCH + H_2$	2.0E07	2.00	15,000	[27]
136.	$CH_2CHCCH + H \rightleftharpoons H_2CCCCH + H_2$	3.0E07	2.00	5000	[27]
137.	$CH_2CHCCH + O \rightleftharpoons HCCO + C_2H_3$	1.4E07	2.00	1900	est[i]
138.	$CH_2CHCCH + O \rightleftharpoons H_2CCCH + HCO$	8.1E06	1.88	180	est[i]
139.	$CH_2CHCCH + OH \rightleftharpoons HCCHCCH + H_2O$	7.5E06	2.00	5000	[27]
140.	$CH_2CHCCH + OH \rightleftharpoons H_2CCCCH + H_2O$	1.0E07	2.00	2000	[27]
141.	$CH_2CHCCH + O_2 \rightleftharpoons HCCHCCH + HO_2$	3.0E13	0.00	60,750	est
142.	$CH_2CHCCH + O_2 \rightleftharpoons H_2CCCCH + HO_2$	3.0E13	0.00	42,200	est
143.	$CH_2CHCHCO + H \rightleftharpoons CH_2CHCH_2 + CO$	6.6E13	−0.02	2740	[35] qrrk
144.	$CH_2CHCHCO + H \rightleftharpoons CH_2CCHCO + H_2$	1.5E07	2.00	6000	est $0.5k_{109}$

(Continued)

Appendix A (Continued)

		A	β	E_a	Source
145.	$CH_2CHCHCO + H \rightleftharpoons CH_2CHCH_2 + CO$	5.9E06	2.00	1300	est[i]
146.	$CH_2CHCHCO + O \rightleftharpoons CH_2HCO + HCCO$	3.0E08	1.45	−860	est $0.5k_{110}$
147.	$CH_2CHCHCO + OH \rightleftharpoons CHCHCHCO + H_2O$	1.0E07	2.00	5000	est $0.5k_{112}$
148.	$CH_2CHCHCO + OH \rightleftharpoons CH_2CCHCO + H_2O$	1.0E07	2.00	2000	est $0.5k_{113}$
149.	$CH_2CHCHCO + OH \rightleftharpoons CH_2CHCH_2 + CO_2$	3.0E12	0.00	0	est[i]
150.	$HCCHCCH(+M) \rightleftharpoons C_4H_2 + H(+M)$	1.0E14	0.00	36,000	[27]
	Low pressure limit:	1.0E14	0.00	30,000	
	Enhanced third-body efficiencies:				
	$H_2O = 5$				
151.	$HCCHCCH + H \rightleftharpoons H_2CCCCH + H$	1.0E14	0.00	0	[27]
152.	$HCCHCCH + OH \rightleftharpoons C_4H_2 + H_2O$	1.0E13	0.00	0	est
153.	$HCCHCCH + O_2 \rightarrow C_2H_2 + CO + HCO$	3.0E12	0.00	0	est, glob
154.	$HCCHCCH + C_2H_2 \rightleftharpoons C_6H_5$	2.8E03	2.90	1400	[27]
155.	$H_2CCCCH(+M) \rightleftharpoons C_4H_2 + H(+M)$	1.0E14	0.00	55,000	[27]
	Low pressure limit:	2.0E15	0.00	48,000	
	Enhanced third-body efficiencies:				
	$H_2O = 5$				
156.	$H_2CCCCH + H \rightleftharpoons C_4H_2 + H_2$	5.0E13	0.00	0	[27]
157.	$H_2CCCCH + O \rightleftharpoons CH_2CO + C_2H$	2.0E13	0.00	0	[27]
158.	$H_2CCCCH + O \rightleftharpoons H_2C_4O + H$	2.0E13	0.00	0	[27]
159.	$H_2CCCCH + OH \rightleftharpoons C_4H_2 + H_2O$	3.0E13	0.00	0	[27]
160.	$H_2CCCCH + O_2 \rightleftharpoons CH_2CO + HCCO$	1.0E12	0.00	0	[27]
161.	$H_2CCCCH + CH_2 \rightleftharpoons C_3H_4 + C_2H$	2.0E13	0.00	0	[27]
162.	$CH_2CCHCO + H \rightarrow H_2CCCH + HCO$	1.0E14	0.00	0	est k_{125}
163.	$CH_2CCHCO + OH \rightarrow CHCCHCO + H_2O$	3.0E13	0.00	0	est k_{126}
164.	$CHCHCHCO \rightleftharpoons H_2CCCH + CO$	6.1E05	0.92	−1120	est[j]
165.	$CHCHCHCO + H \rightleftharpoons CH_2CCHCO + H$	1.0E14	0.00	0	est k_{119}
166.	$CHCHCHCO + H \rightleftharpoons CHCCHCO + H_2$	3.0E07	2.00	1000	est k_{120}
167.	$CHCHCHCO + OH \rightleftharpoons CHCCHCO + H_2O$	2.0E07	2.00	1000	est k_{121}
168.	$CHCHCHCO + O_2 \rightleftharpoons CHCCHCO + HO_2$	1.0E07	2.00	10,000	est k_{122}
169.	$C_4H_2 + H \rightleftharpoons C_4H + H_2$	2.0E07	2.00	2000	[27]
170.	$C_4H_2 + O \rightleftharpoons C_3H_2 + CO$	1.2E12	0.00	0	[27]
171.	$C_4H_2 + OH \rightleftharpoons H_2C_4O + H$	6.7E12	0.00	−410	[27]
172.	$C_4H_2 + OH \rightleftharpoons C_4H + H_2O$	1.0E07	2.00	1000	[27]
173.	$H_2C_4O + H \rightleftharpoons C_2H_2 + HCCO$	5.0E13	0.00	3000	[27]
174.	$H_2C_4O + OH \rightleftharpoons CH_2CO + HCCO$	1.0E07	2.00	2000	[27]
175.	$CHCCHCO + H \rightarrow CHCCCO + H_2$	3.0E07	2.00	5000	est k_{131}
176.	$CHCCHCO + OH \rightarrow CHCCCO + H_2O$	1.0E07	2.00	2000	est k_{135}
177.	$CHCCCO + H \rightarrow C_3H_2 + CO$	5.0E13	0.00	0	est
178.	$CHCCCO + O \rightarrow C_2H + CO + CO$	1.0E13	0.00	0	est
179.	$CHCCCO + OH \rightarrow C_2H_2 + CO + CO$	1.0E13	0.00	0	est
180.	$CHCCCO + O_2 \rightarrow HCCO + CO + CO$	1.0E12	0.00	0	est
181.	$C_4H + O_2 \rightleftharpoons CO + CO + C_2H$	1.0E13	0.00	0	[27]
	C_3 hydrocarbon oxidation subset				
182.	$C_3H_6 + H \rightleftharpoons C_2H_4 + CH_3$	7.2E12	0.00	1300	[73]
183.	$C_3H_6 + H \rightleftharpoons CH_2CHCH_2 + H_2$	1.7E05	2.50	2490	[73]
184.	$C_3H_6 + H \rightleftharpoons CH_2CCH_3 + H_2$	4.1E05	2.50	9800	[73]
185.	$C_3H_6 + H \rightleftharpoons CHCHCH_3 + H_2$	8.0E05	2.50	12,300	[73]
186.	$C_3H_6 + O \rightleftharpoons C_2H_5 + HCO$	1.6E07	1.76	−1216	[73]
187.	$C_3H_6 + O \rightleftharpoons CH_2CHCH_2 + OH$	5.2E11	0.70	5884	[73]
188.	$C_3H_6 + O \rightleftharpoons CHCHCH_3 + OH$	1.2E11	0.70	8960	[73]
189.	$C_3H_6 + O \rightleftharpoons CH_2CCH_3 + OH$	6.0E10	0.70	7630	[73]
190.	$C_3H_6 + OH \rightleftharpoons CH_2CHCH_2 + H_2O$	3.1E06	2.00	−298	[73]
191.	$C_6H_6 + OH \rightleftharpoons CH_2CCH_3 + H_2O$	1.1E06	2.00	1451	[73]

(Continued)

Appendix A (Continued)

		A	β	E_a	Source
192.	$C_3H_6 + OH \rightleftharpoons \dot{C}HCHCH_3 + H_2O$	2.1E06	2.00	2778	[73]
193.	$C_3H_6 + HO_2 \rightleftharpoons CH_2CH\dot{C}H_2 + H_2O_2$	9.6E03	2.60	13,909	[73]
194.	$C_3H_6 + O_2 \rightleftharpoons \dot{C}H_2CHCH_2 + HO_2$	2.0E13	0.00	47,600	[73]
195.	$C_3H_6 + O_2 \rightleftharpoons \dot{C}HCHCH_3 + HO_2$	2.0E13	0.00	47,600	[73]
196.	$C_3H_6 + O_2 \rightleftharpoons CH_2\dot{C}CH_3 + HO_2$	2.0E13	0.00	47,600	[73]
197.	$CH_2CH\dot{C}H_2 + H \rightleftharpoons H_2CCCH_2 + H_2$	5.0E13	0.00	0	[28]
198.	$CH_2CH\dot{C}H_2 + H \rightleftharpoons C_3H_6$	1.9E26	−3.60	5470	[28]
199.	$CH_2CH\dot{C}H_2 + O \rightleftharpoons CH_2CHCHO + H$	1.8E14	0.00	0	[28]
200.	$CH_2CH\dot{C}H_2 + OH \rightleftharpoons H_2CCCH_2 + H_2O$	1.0E13	0.00	0	[73]
201.	$CH_2CH\dot{C}H_2 + HO_2 \rightleftharpoons CH_2CHCHO + H + OH$	1.0E13	0.00	0	[73]
202.	$CH_2CH\dot{C}H_2 + O_2 \rightleftharpoons CH_2CHCHO + OH$	1.8E13	−0.41	22,860	[28]
203.	$CH_2CH\dot{C}H_2 + O_2 \rightleftharpoons H_2CCCH_2 + HO_2$	5.0E15	−1.40	22,430	[28]
204.	$CH_2CH\dot{C}H_2 + O_2 \rightleftharpoons CH_2HCO + CH_2O$	1.1E10	0.34	12,840	[28]
205.	$\dot{C}H_2CHCH_2 + O_2 \rightleftharpoons C_2H_2 + CH_2O + OH$	2.8E25	−4.80	15,470	[28]
206.	$\dot{C}HCHCH_3 + H \rightleftharpoons CH_2CH\dot{C}H_2 + H$	1.0E14	0.00	0	[28]
207.	$\dot{C}HCHCH_3 + H \rightleftharpoons H_3CCCH + H_2$	2.0E13	0.00	0	[28]
208.	$\dot{C}HCHCH_3 + OH \rightleftharpoons H_3CCCH + H_2O$	1.0E13	0.00	0	[28]
209.	$\dot{C}HCHCH_3 + O_2 \rightleftharpoons CH_3HCO + HCO$	1.1E23	−3.29	3900	[28]
210.	$CH_2\dot{C}CH_3 + H \rightleftharpoons CH_2CH\dot{C}H_2 + H$	1.0E14	0.00	0	[28]
211.	$CH_2\dot{C}CH_3 + H \rightleftharpoons H_3CCCH + H_2$	4.0E13	0.00	0	[28]
212.	$CH_2\dot{C}CH_3 + O \rightleftharpoons CH_2CO + CH_3$	1.0E14	0.00	0	[28]
213.	$CH_2\dot{C}CH_3 + OH \rightleftharpoons H_3CCCH + H_2O$	2.0E13	0.00	0	[28]
214.	$CH_2\dot{C}CH_3 + O_2 \rightleftharpoons CH_3CO + CH_2O$	1.1E22	−3.29	3900	[28]
215.	$H_2CCCH_2 \rightleftharpoons CH_3CCH$	2.2E14	0.00	68,100	[28]
216.	$H_2CCCH_2 + H \rightleftharpoons CH_3CCH + \dot{H}$	1.0E13	0.00	5000	[27]
217.	$H_2CCCH_2 + H(+M) \rightleftharpoons CH_2CH\dot{C}H_2(+M)$	1.2E11	0.69	3000	[28]
	Low pressure limit:	5.6E33	−5.00	4450	
	Troe parameters: 0.7086 134 1784 5740				
218.	$H_2CCCH_2 + H(+M) \rightleftharpoons CH_2\dot{C}CH_3(+M)$	8.5E12	0.00	2000	[28]
	Low pressure limit:	1.1E34	−5.00	4450	
	Troe parameters: 0.7086 134 1784 5740				
219.	$H_2CCCH_2 + O \rightleftharpoons C_2H_4 + CO$	1.3E07	1.88	180	[28]
220.	$H_2CCCH_2 + H \rightleftharpoons H_2CC\dot{C}H + H_2$	3.0E07	2.00	5000	[27]
221.	$H_2CCCH_2 + OH \rightleftharpoons H_2C\dot{C}CH + H_2O$	2.0E07	2.00	1000	[27]
222.	$CH_3CCH + H \rightleftharpoons H_2C\dot{C}CH + H_2$	3.0E07	2.00	5000	[27]
223.	$CH_3CCH + H \rightleftharpoons CH_3 + C_2H_2$	1.0E14	0.00	4000	[27]
224.	$CH_3CCH + H(+M) \rightleftharpoons CH_2\dot{C}CH_3(+M)$	6.5E12	0.00	2000	[28]
	Low pressure limit:	8.5E39	−7.27	6580	
	Troe parameters: 0.7086 134 1784 5740				
225.	$CH_3CCH + OH \rightleftharpoons H_2C\dot{C}CH + H_2O$	2.0E07	2.00	1000	[27]
226.	$CH_3CCH + O \rightleftharpoons C_2H_4 + CO$	1.5E13	0.00	2100	[28]
227.	$CH_2CHCHO + H \rightleftharpoons C_2H_4 + HCO$	2.0E13	0.00	3500	[28]
228.	$CH_2CHCHO + H \rightleftharpoons CH_2CH\dot{C}O + H_2$	4.0E13	0.00	4200	[28]
229.	$CH_2CHCHO + O \rightleftharpoons CH_2CH\dot{C}O + OH$	7.2E12	0.00	1970	[28]
230.	$CH_2CHCHO + O \rightleftharpoons CH_2CO + HCO + H$	5.0E07	1.76	76	[28]
231.	$CH_2CHCHO + OH \rightleftharpoons CH_2CH\dot{C}O + H_2O$	1.0E13	0.00	0	[28]
232.	$CH_2CH\dot{C}HO + O_2 \rightleftharpoons CH_2CH\dot{C}O + HO_2$	3.0E13	0.00	36,000	[28]
233.	$H_2C\dot{C}CH + H(+M) \rightleftharpoons H_2CCCH_2(+M)$	1.0E17	−0.82	315	[27]
	Low pressure limit:	3.5E55	−4.88	2225	
	Troe parameters: 0.7086 134 1784 5740				
	Enhanced third-body efficiencies:				
	H_2O = 8.6				
234.	$H_2C\dot{C}CH + H(+M) \rightleftharpoons CH_3CCH(+M)$	1.0E17	−0.82	315	[27]
	Low pressure limit:	3.5E55	−4.88	2225	
	Troe parameters: 0.7086 134 1784 5740				

(Continued)

Appendix A (Continued)

		A	β	E_a	Source
	Enhanced third-body efficiencies: $H_2O = 8.6$				
235.	$H_2CC\dot{C}H + H \rightleftharpoons C_3H_2 + H_2$	5.0E13	0.00	1000	[27]
236.	$H_2CC\dot{C}H + O \rightleftharpoons CH_2O + C_2H$	1.4E14	0.00	0	[27]
237.	$H_2CC\dot{C}H + OH \rightleftharpoons C_3H_2 + H_2O$	2.0E13	0.00	0	[27]
238.	$H_2CC\dot{C}H + O_2 \rightleftharpoons CH_2CO + HCO$	3.0E10	0.00	2868	[27]
239.	$H_2CC\dot{C}H + H_2CC\dot{C}H \rightleftharpoons C_6H_5 + H$	1.0E13	0.00	0	[27]
240.	$CH_2CH\dot{C}O \rightleftharpoons C_2H_3 + CO$	1.0E14	0.00	34,000	[28]
241.	$CH_2CH\dot{C}O + O \rightleftharpoons C_2H_3 + CO_2$	1.0E14	0.00	0	[28]
242.	$CH_2CH\dot{C}O + O_2 \rightleftharpoons CH_2HCO + CO_2$	5.4E20	−2.72	7000	[35] qrrk
243.	$C_3H_2 + O \rightleftharpoons C_2H_2 + CO$	1.0E14	0.00	0	[27]
244.	$C_3H_2 + OH \rightleftharpoons C_2H_2 + HCO$	5.0E13	0.00	0	[27]
245.	$C_3H_2 + O_2 \rightleftharpoons HCCO + CO + H$	2.0E12	0.00	1000	[27]
246.	$C_3H_2 + CH_3 \rightleftharpoons CH_2\dot{C}HCCH + H$	2.0E13	0.00	0	[27]
247.	$C_3H_2 + HCCO \rightleftharpoons H\dot{C}CHCCH + CO$	3.0E13	0.00	0	[27]
248.	$C_3H_2 + H_2CC\dot{C}H \rightleftharpoons C_6H_4 + H$	1.0E13	0.00	0	[27]
249.	$O_2CCHO\dot{O} \rightleftharpoons HCOO + CO_2$	3.0E13	0.00	4000	[35] est

[a] In the mechanism, no distinction is made between isomers of the cyclic compounds C_5H_5O, C_5H_5OH, and C_5H_7.
[b] Estimated by analogy to C_6H_6 reactions.
[c] Estimated by analogy to C_3H_x hydrocarbon reactions ($x = 5–8$).
[d] Estimated by analogy to CH_3OH or C_2H_5OH reactions.
[e] Lumped reaction, assuming rapid dissociation of cyclobutadiene.
[f] To bring the rate constant in accordance with the revised heat of formation for C_5H_4O, the activation energy was raised by 6 kcal/mol.
[g] Estimated by analogy to CH_2O reactions.
[h] Based on estimate for $CH_2CHCH\dot{C}HO \rightarrow CH_2C\dot{H}CH_2 + CO$ [35].
[i] Estimated by analogy to C_2 hydrocarbon reactions (C_2H_4, C_2H_2, or CH_2CO).
[j] Based on estimate for $CH_2CHCH_2\dot{C}O \rightleftharpoons H_2CC\dot{C}H + CO$ [35].
For "duplicate reactions" the resulting rate constant is the sum of the rate constants listed.

(not shown) and CO are significantly underpredicted. These deviations may partly be attributed to the difference in temperature for observed and predicted onset of benzene oxidation. Furthermore, the uncertainty in the overall oxidation pathways for benzene at these temperatures and the probability of missing consumption steps in the mechanism will affect the predictions for benzoquinone and cyclopentadienone. However, the large discrepancy observed for phenol is difficult to understand. The jet-stirred-reactor data appear to be incompatible with the flow-reactor data of Figure 7, which are fairly well predicted by the mechanism. Phenol is formed and consumed by the same reactions under well-mixed conditions as under flow-reactor conditions (Fig. 4), even though the relative importance of reactions is slightly different due to differences in the concentration and composition of the radical pool. With a few exceptions, these reactions are fairly well characterized and we were not able to obtain agreement between the measured and calculated phenol profile by adjusting any of these steps within their uncertainty limits. Further work is required to resolve this issue.

CONCLUSIONS

The oxidation of benzene has been studied in an isothermal flow reactor at atmospheric pressure and temperatures in the range 900–1400 K. The excess-air ratio was varied from close to stoichiometric to very lean conditions. In addition, the radical pool composition was perturbed by varying the levels of water vapor (0.5 to 5%) and by adding NO (0 and 100 ppm). The results were analyzed in terms of a detailed chemical kinetic model, which has been developed in this work.

Results indicate that the oxidation rate of benzene is mainly controlled by temperature and stoichiometry. The onset of oxidation occurs at ~1000 K; complete oxidation occurs between 1100 and 1300 K, depending on the stoichiometry. Under lean conditions, presence of NO further lowers the initiation temperature by 60–80 K. The effect of the OH/O ratio is less important.

A chemical kinetic model for benzene oxidation has been developed. It was evaluated by comparison with experimental data from the present work as well as flow-reactor and mixed-reactor data from literature.

Appendix B Thermodynamic Properties for Selected Species

Species	ΔH_{f298}	S_{298}	C_{p300}	C_{p400}	C_{p500}	C_{p600}	C_{p800}	C_{p1000}	C_{p1500}	Source
C_6H_6	19.81	64.35	19.92	27.09	33.25	38.38	45.87	51.05	58.31	[30]
C_6H_5	80.73	69.82	21.01	27.06	32.43	37.05	43.90	47.77	53.26	[30,26]
C_6H_4	121.76	69.53	18.61	24.33	29.19	33.19	38.90	42.81	48.24	[30]
C_6H_5O	10.35	74.87	24.79	31.31	37.08	42.01	49.25	53.28	58.98	[30]
C_6H_5OH	−25.01	76.93	25.43	32.11	38.09	43.28	51.12	55.68	62.24	[30]
p-OC_6H_4O	−29.37	79.62	26.04	32.20	37.67	42.27	48.87	53.42	59.48	[31]
o-OC_6H_4O[a]	−25.00									[74]
OC_6H_3O	27.03	77.15	24.86	31.62	37.21	41.37	47.25	51.64		[35]
C_5H_7	39.88	73.65	19.23	26.40	32.57	37.64	44.82	49.77	57.31	[31]
C_5H_6	31.99	64.45	16.67	23.12	28.70	33.39	40.31	45.10	51.82	[30]
C_5H_5	62.00	59.43	34.75	36.13	37.46	38.75	41.18	43.39	47.92	[23,30]
C_5H_5O	42.94	72.73	20.61	27.19	32.59	36.99	43.45	47.72	53.79	[18]
C_5H_5OH	−9.02	75.33	22.09	29.03	34.71	39.34	46.16	50.71	57.40	[18]
C_5H_4O	13.20	66.49	19.70	25.79	30.69	34.62	40.25	43.90	49.00	[23,31]
C_5H_4OH	15.90	74.08	22.98	29.34	34.50	38.52	43.83	47.57	52.86	[23,31]
C_5H_4	131.79	66.81	17.60	22.64	27.00	30.53	35.25	38.60	43.20	[31]
C_5H_3O	68.95	69.20	18.69	24.13	28.51	32.04	37.09	40.34	44.70	[35]
C_5H_3	166.75	67.32	17.04	21.74	25.59	28.60	32.48	35.15	38.73	[31]
$CH_2\dot{C}HCHCHCH_3$	18.19	76.48	24.23	30.73	36.36	41.10	47.91	51.19	60.25	[31]
$CH_2CH\dot{C}HCHCH_2$	49.31	75.93	21.07	27.67	33.14	37.68	44.57	49.43	56.81	[17]
$CH_2CHCH\dot{C}HCH_2$	49.11	77.20	22.52	29.00	34.25	38.56	45.20	50.19	57.42	[17]
$CHCCH\dot{C}HCH_2$	97.09	73.38	21.94	27.24	31.43	34.80	39.89	43.18	48.29	[31]
$CH_2CH\dot{C}HCHCHOH$	7.18	85.00	25.02	32.27	38.09	42.76	49.62	54.33	61.52	[17]
$CH_2CHCHCH\dot{C}H_2OH$	−16.25	87.20	27.68	34.31	39.88	44.55	51.79	57.03	65.21	[35]
$CHOCH_2CH_2\dot{C}HCHO$	−27.18	102.84	30.36	35.62	40.36	44.59	51.63	56.94	64.64	[35]
$CH_2CH\dot{C}HCH_2$	28.29	70.44	18.58	23.16	27.42	31.26	37.44	41.29	46.79	[30]
$CH_2CH\dot{C}CH_2$	74.14	75.31	19.49	23.12	26.47	29.48	34.32	37.37	41.84	[30]
$CH_2CHCH\dot{C}H$	86.09	73.06	19.38	23.47	27.21	30.54	35.79	38.89	43.16	[30]
CH_2CHCCH	69.14	67.33	17.32	20.61	23.62	26.30	30.53	33.20	37.25	[30]
$HCCHCCH$	129.88	69.06	18.02	20.82	23.29	25.41	28.56	30.46	33.46	[30]
H_2CCCCH	111.32	72.94	20.24	22.43	24.44	26.23	29.10	30.93	33.68	[30]
$CHOCH_2CH_2\dot{C}HO$	−68.60	87.61	26.38	30.97	35.03	38.61	44.46	48.88	55.45	[35]
$CHOCH_2\dot{C}H_2CO$	−31.70	90.11	25.55	29.54	33.07	36.19	41.31	45.17	50.88	[35]
$CH_2C\dot{H}CHCHO$	15.45	76.87	19.43	24.28	28.43	31.96	37.47	41.38	46.93	[18]
$CH_2CHCH_2\dot{C}O$	18.85	81.79	20.18	24.69	28.55	31.85	37.05	40.80	46.33	[35]
$\dot{C}H_2CHCHCO$	1.82	71.96	21.66	26.31	29.92	32.71	36.53	38.95	43.25	[18]
$\dot{C}HCHCHCO$	60.92	73.81	21.99	26.19	29.09	31.08	33.65	35.66	38.78	[35]
H_2C_4O	54.59	66.43	17.27	19.62	21.79	23.73	26.81	28.73	31.51	[30]
$CH_2CH\dot{C}H_3$	4.89	61.51	15.46	19.27	22.73	25.80	30.78	34.52	40.14	[30]
$CH_2\dot{C}HCH_2$	38.64	64.73	16.07	19.55	22.72	25.53	29.99	32.89	37.43	[30]
$\dot{C}H_2CCH_3$	61.09	69.24	15.45	18.38	21.21	23.89	28.50	31.60	36.09	[30]
$\dot{C}HCHCH_3$	64.75	68.74	15.54	18.56	21.44	24.12	28.65	31.68	36.13	[30]
H_2CCCH_2	47.63	57.94	14.25	16.97	19.46	21.71	25.45	28.20	32.06	[30]
H_3CCCH	45.77	58.89	14.51	17.06	19.40	21.54	25.16	27.90	31.79	[30]
H_2CCCH	83.04	61.48	15.84	17.74	19.47	21.01	23.43	25.00	27.55	[30]
C_3H_2	129.60	64.81	14.93	16.10	16.91	17.55	18.72	19.74	21.22	[30]
CH_2CHCHO	−20.32	67.39	16.98	20.89	24.09	26.70	30.57	33.22	37.44	[18]
$\dot{C}HOCHCHOH$	−62.45	76.87	20.40	24.07	27.22	29.89	34.09	37.11	41.57	[35]
$\dot{C}HCHC\dot{H}O$	38.78	69.24	17.48	20.61	23.12	25.11	27.94	29.76	32.54	[18]
$CH_2CH\dot{C}O$	10.58	68.07	15.91	19.28	22.00	24.19	27.37	29.47	32.73	[18]
$O_2\dot{C}CHO\dot{O}$	−61.69	88.68	21.91	23.72	25.54	27.29	30.33	32.54	34.45	[35]

[a] As an approximation, entropy and heat of formation for orthobenzoquinone were assumed similar to parabenzoquinone.

The model provides a fairly good description of the overall oxidation behavior of benzene over the range of conditions investigated. Thereby, the mechanism can be used with some confidence to simulate benzene oxidation under postflame conditions. However, a number of kinetic issues need to be addressed before concentrations of cyclic and linear intermediates can be predicted satisfactorily. These include rate and product channels for the reactions of phenyl and cyclopentadienyl with molecule oxygen as well as reaction chemistry for the oxygenated cyclic C_6 and C_5 compounds.

The authors would like to thank Professor J. W. Bozzelli for sharing results on aromatics chemistry prior to publication. The work was carried out as part of the combustion research program of the Department of Chemical Engineering of the Technical University of Denmark (CHEC). The CHEC research program is cofunded by the Danish Technical Research Council, Elsam, Elkraft, and the Danish Ministry of Energy. M. U. Alzueta acknowledges CAI and CONSID for the "Ayuda Europa" awarded for carrying out part of this research. In addition, the work was funded by the Human Capital and Mobility program of the European Union (Contract No. CHRX-CT94-0436).

BIBLIOGRAPHY

1. Bittner, J. D.; Howard, J. B. Eighteenth Symposium (International) on Combustion; The Combustion Institute: Pittsburgh, PA, 1981; p 1105.
2. Venkat, C.; Brezinsky, K.; Glassman, I. Nineteenth Symposium (International) on Combustion; The Combustion Institute: Pittsburgh, PA, 1982; p 143.
3. Hsu, H.; Lin, C. Y.; Lin, M. C. Twentieth Symposium (International) on Combustion; The Combustion Institute: Pittsburgh, PA, 1984; p 623.
4. Brezinsky, K. Prog Energy Combust Sci 1986, 12, 1.
5. Burcat, A.; Snyder, C.; McBride, B. J. Ignition delay times of benzene and toluene with oxygen in argon mixtures; NASA TM-87312, 1986.
6. Lovell, A. B.; Brezinsky, K.; Glassman, I. Twenty-Second Symposium (International) on Combustion; The Combustion Institute: Pittsburgh, PA, 1988; p 1063.
7. Lyon, R. K. Twenty-Third Symposium (International) on Combustion; The Combustion Institute: Pittsburgh, PA, 1990; p 903.
8. Bittker, D. A. Combust Sci Techn 1991, 79, 49.
9. Emdee, J. L.; Brezinsky, K.; Glassman, I. J. Phys Chem 1992, 96, 2151.
10. Lindstedt, R. P.; Skevis, G. Combust Flame 1994, 99, 551.
11. Leung K. M.; Lindstedt, R. P. Combust Flame 1995, 102, 129.
12. Zhang, H.-Y.; McKinnon, J. T. Combust Sci Techn 1995, 107, 261.
13. Lindstedt, R. P.; Maurice, L. Q. Combust Sci Techn 1996, 120, 119.
14. Tan, Y.; Frank, P. Twenty-Sixth Symposium (International) on Combustion; The Combustion Institute: Pittsburgh, PA, 1996; p 677.
15. Shandross, R. A. S.; Lovell, J. P.; Howard, J. B. Twenty-Sixth Symposium (International) on Combustion; The Combustion Institute: Pittsburgh, PA, 1996; p 711.
16. Davis, S. G.; Wang, H.; Brezinsky, K.; Law, C. K. Twenty-Sixth Symposium (International) on Combustion; The Combustion Institute: Pittsburgh, PA, 1996; p 1025.
17. Zhong, X.; Bozzelli, J. W. Int J Chem Kinet 1997, 29, 893.
18. Zhong, X.; Bozzelli, J. W. J Phys Chem A 1998, 102, 3537.
19. Chai, Y.; Pfefferle, L. D. Fuel 1998, 77, 313.
20. Frank, P.; Herzler, J.; Just, Th.; Wahl, C. Twenty-Fifth Symposium (International) on Combustion; The Combustion Institute: Pittsburgh, PA, 1994; p 833.
21. Kumaran, S. S.; Michael, J. V. In Phenyl Radical Thermolysis and Rate Constants for Phenyl + O_2, Proceedings of the 21st International Symposium on Shock Waves, Great Keppel Island, Australia, 1997.
22. Alzueta, M. U.; Oliva, M.; Glarborg, P. Int J Chem Kinet 1998, 30, 683.
23. Wang, H.; Brezinsky, K. J. Phys Chem A 1998, 102, 1530.
24. Miller, J. A.; Melius, C. F. Combust Flame 1992, 91, 21.
25. Baulch, D. C.; Cobos, C. J.; Cox, R. A.; Esser, C.; Frank, P.; Just, T.; Kerr, J. A.; Pilling, M. J.; Troe, J.; Walker, R. W.; Warnatz, J. J. Phys Chem Ref Data 1992, 21, 411.
26. Baulch, D. C.; Cobos, C. J.; Cox, R. A.; Frank, P.; Hayman, C.; Just, T.; Kerr, J. A.; Pilling, M. J.; Troe, J.; Walker, R. W.; Warnatz, J. Combust Flame 1994, 98, 59.
27. Pauwels, J.-F.; Volponi, J. V.; Miller, J. A. Combust Sci Techn 1995, 110, 249.
28. Marinov, N. M.; Pitz, W. J.; Westbrook, C. K.; Castaldi, M. J.; Senkan, S. M. Combust Sci Techn 1996, 116, 211.
29. Glarborg, P.; Alzueta, M. U.; Dam-Johansen K.; Miller, J. A. Combust Flame 1998, 115, 1.
30. Kee, R. J.; Rupley, F. M.; Miller, J. A. The Chemkin Thermodynamic Data Base, Sandia Report SAND87-8215; Sandia National Laboratories: Livermore, CA, 1991.
31. Burcat, A.; McBride, B. 1995 Ideal Gas Thermodynamic Data for Combustion and Air-Pollution Use, Aerospace Engineering Report TAE 732; Institute of Technology: Technian, Israel, 1995 and updates.
32. Kristensen, P. G.; Glarborg, P.; Dam-Johansen, K. Combust Flame 1996, 107, 211.
33. Alzueta, M. U.; Glarborg, P.; Dam-Johansen, K. Combust Flame 1997, 109, 25.

34. Alzueta, M. U.; Røjel, H.; Kristensen, P.; Glarborg, P.; Dam-Johansen, K. Energy Fuels 1997, 11, 716.
35. Bozzelli, J. Private communication of preliminary results. See also Zhong, X. Ph.D. Thesis, Rutgers University: Newark, NJ, May 1998.
36. Heckmann, E.; Hippler, H.; Troe, J. Twenty-Sixth Symposium (International) on Combustion; The Combustion Institute: Pittsburgh, PA, 1996; p 543.
37. Mebel, A. M.; Lin, M. C.; Yu, T.; Morokuma, K. J. Phys Chem A 1997, 101, 3189.
38. Nicovich, J. M.; Gump, C. A.; Ravishankara, A. R. J Phys Chem 1982, 86, 1684.
39. Bajaj, P. N.; Fontijn, A. Combust Flame 1996, 105, 239.
40. Leidreiter, H. I.; Wagner, H. Gg. Z Phys Chem (Neue Folge) 1989, 165, 1.
41. Frenklach, M.; Clary, D. W.; Yuan, T.; Gardiner, W. C. Stein, S. E. Combust Sci Techn 1986, 50, 79.
42. Castaldi, M. C.; Marinov, N. M.; Melius, C. F.; Huang, J.; Senkan, S. M.; Pitz, W.; Westbrook, C. K. Twenty-Fifth Symposium (International) on Combustion; The Combustion Institute: Pittsburgh, PA, 1994; p 693.
43. Lin, C. Y.; Lin, M. C. J Phys Chem 1986, 90, 425.
44. Mebel, A. M.; Lin, M. C. J Am Chem Soc 1994, 116, 9577.
45. Yu, T.; Lin, M. C. J Am Chem Soc 1994, 116, 9571.
46. Tranter, R. S.; Grotheer, H. H.; Just, Th. Fourteenth International Gas Kinetics Symposium, Leeds 1996, paper F7.
47. Knispel, R.; Koch, R.; Siese, M.; Zetzsch, C. Ber Bunsenges Phys Chem 1990, 94, 1375.
48. Horn, C.; Roy, K.; Frank, P.; Just, Th. Twenty-Seventh Symposium (International) on Combustion; The Combustion Institute: Pittsburgh, PA, 1998; p 321.
49. Olivella, S.; Solè, A.; Garcia-Raso, A. J Phys Chem 1995, 99, 10549.
50. Liu, R.; Morokuma, K.; Mebel, A. M.; Lin, M. C. J Phys Chem 1996, 100, 9314.
51. Buth, R.; Hoyermann, K.; Seeba, J. Twenty-Fifth Symposium (International) on Combustion; The Combustion Institute: Pittsburgh, PA, 1994; p 841.
52. Lin, M. C.; Mebel, A. M. J Phys Org Chem 1995, 8, 407.
53. de Jongh, D. C.; van Fossen, R. Y., Bourgeois, C. F. Tetrahedron Lett 1967, 3, 271.
54. Schraa, G.-J.; Arends, I. W. C. E.; Mulder, P. J Chem Soc Perkin Trans 1994, 2, 189.
55. Sakai, T.; Hattori, M.; Yamane, N. J. Japan Petrol Int 1980, 23, 44.
56. Roy, K.; Frank, P. Twenty-First International Symposium on Shock Waves, Great Keppel Island, Australia, 1997, paper 1560.
57. Horn, C.; Roy, K.; Frank, P.; Slutsky, V.; Just, Th. Twenty-Seventh Symposium (International) on Combustion; The Combustion Institute: Pittsburgh, PA, 1998; p 329.
58. Burcat, A.; Dvinyaninov, M. Int J Chem Kinet 1997, 29, 505.
59. Bruinsma, O-S. L.; Tromp, P. J. J.; de Sauvage Nolting, H. J. J.; Moulijn, J. A. Fuel 1988, 67, 334.
60. Lutz, A. E.; Kee, R. J.; Miller, J. A. SENKIN: A Fortran Program for Predicting Homogeneous Gas Phase Chemical Kinetics with Sensitivity Analysis, Sandia Report SAND87-8248; Sandia National Laboratories: Livermore, CA, 1987.
61. Glarborg, P.; Kee, R. J.; Grcar, J. F.; Miller; J. A. PSR: A Fortran Program for Modeling Well-Stirred Reactors, Sandia Report SAND86-8209; Sandia National Laboratories: Livermore, CA, 1986.
62. Kee, R. J.; Rupley, F. M.; Miller J. A. CHEMKIN-II: A Fortran Chemical Kinetics Package for the Analysis of Gas-Phase Chemical Kinetics, Sandia Report SAND89-8009; Sandia National Laboratories: Livermore, CA, 1989.
63. He, Y. Z.; Mallard, W. G.; Tsang, W. J Phys Chem 1988, 92, 2196.
64. Cyprès, R.; Bettens, B. Tetrathedron 1974, 30, 1253.
65. Brezinsky, K.; Pecullan, M.; Glassman, I. J Phys Chem A 1998, 102, 8614.
66. Hjuler, K.; Glarborg, P.; Dam-Johansen, K. Ind Engn Chem Res 1995, 34, 1882.
67. Glarborg, P.; Kristensen, P. G.; Kubel, D.; Hansen, J.; Dam-Johansen, K. Combust Sci Techn 1995, 110−111, 46.
68. Alzueta, M. U.; Muro, J.; Bilbao, R.; Glarborg, P. Israel J Chem 1999, 39, 73.
69. Bendtsen, A. B.; Glarborg, P.; Dam-Johansen, K. Combust Sci Technol 2000, 151, 31−72.
70. Ackerman, L.; Hippler, H.; Reihs, C.; Troe, J. J Phys Chem 1990, 94, 5247.
71. Fahr, A.; Stein, S. E. J Phys Chem 1988, 92, 4951.
72. Arends, I. W. C. E.; Louw, R.; Mulder, P. J Phys Chem 1993, 97, 7914.
73. Tsang, W. J Phys Chem Ref Data 1991, 20, 221.
74. Lias, S. G.; Liebman, J. F.; Levin, R. D.; Kafafi, S. A. NIST Standard Reference Database 25: Structures and Properties, version 2.02, 1994.